

國立成功大學
機械工程學系
碩士論文

可自行平衡具十連桿型腿部機構四足步行機器之設計

On the Design of
A Self-Balanced Quadruped Walking Machine
with 10-bar Leg Mechanisms

研究生：黃智勇 Chih-Yung Huang
指導教授：顏鴻森 Hong-Sen Yan

Thesis for the Degree of Master of Science
Department of Mechanical Engineering
National Cheng Kung University
May 2006

中華民國九十五年五月

國立成功大學
碩士論文

可自行平衡具十連桿型腿部機構
四足步行機器之設計

On the Design of
A Self-Balanced Quadruped Walking Machine
With 10-bar Leg Mechanisms

研究生：黃智勇

本論文業經審查及口試合格特此證明

論文考試委員

顏鴻森

藍明俊
李俊傑

指導教授：顏鴻森

系(所)主管：張錦福

中華民國九十五年五月二十五日

摘要

本研究的主要目的為, 利用一套系統化的方法, 設計出具有十連桿組的腿部機構, 可自行平衡行走的四足步行機器。首先, 挑選一個現存的十連桿腿部機構作為初始設計, 並利用 ALM 最佳化方法針對這個腿部機構進行尺寸合成, 得到理想的足部軌跡曲線。接著, 利用二段式速度控制的概念, 調整腿部機構在支撐相與轉換相之間的時間比, 增長腿部機構在支撐相的時間。然後, 為了保持此步行機器隨時至少有三條腿接觸地面以加強移動時的穩定性, 在某特定時間四條腿的足點都安置在特定的位置, 以保持此波浪型步態相位差。再來, 針對所設計出的步行機器, 分析與評估其特性, 包括運動分析、力量分析、以及電腦動畫模擬。運動分析顯示, 最佳化設計後之腿部機構在跨越性能上有良好的表現。在力量分析方面, 藉由機械利益推估得知此步行機器雖然不具機械利益為零的死點位置, 但是會在交換懸空腿時發生機械利益劇降的情形。藉由動畫模擬的製作, 可避免此步行機器在作動時, 腿部機構的桿件發生干涉, 並確定運動時各腿足點在預期之位置。最後, 製作出此四足步行機器之原型機, 並驗證出本設計是可行的。

關鍵字詞：四足步行機器、連桿機構、尺寸合成、最佳設計

ABSTRACT

A self-balanced quadruped walking machine with leg mechanisms of 10-bar linkage is designed by a systematic approach. At first, an existing leg mechanism of 10-bar linkage is selected as the tentative design, and the dimensional synthesis is performed to obtain the desired foot trajectory by the optimization technique of ALM. Next, the time ratio between the support phase and the transfer phase is adjusted by a two-speed control method to increase the time period of support phase. Then, in order to make sure that there are always at least three legs on the ground for the wave gait to enhance the stability of locomotion, the foot point of each leg at a specific time is placed on the specific position upon the foot trajectory. The kinematic analysis, force analysis, simulation, and animation are carried out to evaluate the characteristics of the designed walking machine. The kinematic analysis reveals that after optimum design, the designed leg mechanism has a good stability for striding. The force analysis shows that this walking machine does not run into the configuration of dead center position with the mechanical advantage of zero. However, the mechanical advantage suddenly drops down while the walking machine changes the transferring leg during the locomotion. From the simulation and animation, we know that there is no interference between the links of the leg mechanism and that the foot point positions of each leg are at the expected positions during the locomotion. Finally, a prototype of the designed quadruped walking machine is constructed and it is proven that this design is practical and feasible.

Keyword: quadruped walking machine, linkage mechanism, dimensional synthesis, optimal design

ACKNOWLEDGEMENTS

Without encouragement and help from the persons of importance for me, I would never have been able to accomplish this thesis. I will here express my greatest appreciation to them for their inspiration and support in all sincerity.

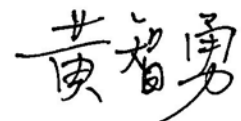
First of all, I would like to express my sincere appreciation to my advisor, Prof. Hong-Sen Yan, who offered me the sage advice and criticisms for my thesis, and provided me with the valuable guidance, constant encouragement, and financial support in the past two years. Without the great help from Prof. Yan, I would not get through with my master program completely.

I am grateful to acknowledge my thesis committee, including Prof. Ming-June Tsai and Prof. Chao-Chieh Lan from National Cheng Kung University, for their worthwhile and insightful suggestions to this work.

I also wish to thank all of my former and present fellows in the Creative Machine Design Education & Research Laboratory at National Cheng Kung University, who are Dr. Nien-Te Liu, Dr. Chia-Chun Chu, Dr. Hsing-Hui Huang, Dr. Domenico Mundo, Dr. Feng-Ming Ou, Dr. Yi-Chang Wu, and Dr. Hsin-Te Wang, the seniors, Jun-Wei, Guo-Jih, Chih-Ching, Kuo-Hong, Chen-Hsiung, Wu-Jung, Yu-Ju, Chin-Hsing, Jen-Chih, Jung-Chan, Kao-Chu, and Shao-Hung, my dear classmate, Guo-Bin, the juniors, Feng-Yuan, Yi-Ming, and Shao-Ying, and the assistants, Yu-Ling and Hsi-Yen. I appreciate the help I have received from them and I enjoyed the experience of working with them for these years.

Finally, I deeply appreciated my parents for their profoundest love and continuous support since I was born. Also, thanks to my sister and brother. In addition, I would like to thank my girlfriend, Chia Yi, for her patience and encouragement. This thesis is cordially devoted to all of them.

I am sorry if I have missed someone on my list, but you all have been great help.



Chih-Yung Huang

June 2006

TABLE OF CONTENTS

摘要(ABSTRACT in Chinese)	I
ABSTRACT	II
ACKNOWLEDGEMENTS	III
TABLE OF CONTENTS	IV
LIST OF TABLES	VII
LIST OF FIGURES	VIII
CHAPTER 1 INTRODUCTION	1
1.1 FEATURES OF WALKING MACHINES	1
1.2 LITERATURE SURVEY	2
1.3 MOTIVATIONS AND OBJECTIVES	6
1.4 ORGANIZATION OF THESIS	6
CHAPTER 2 GAIT AND FOOT TRAJECTORY	9
2.1 BASIC DEFINITIONS	9
2.2 GAIT ANALYSIS	11
2.2.1 Gaits of Quadruped Animals	11
2.2.2 Graphic Methods of Gait Analysis	14
2.3 FOOT TRAJECTORY	15
2.4 SUMMARY	17
CHAPTER 3 DESIGN APPROACH	18
3.1 DESIGN PROCEDURE	18
3.2 EXISTING PATH GENERATORS	20
3.3 USABLE LEG MECHANISMS	22
3.3.1 Position Analysis	22
3.3.2 Dimensional Synthesis	26

3.4 FEASIBLE LEG MECHANISMS.....	30
3.5 PLACEMENT OF FOOT-POINT POSITIONS.....	31
3.6 SUMMARY.....	33
CHAPTER 4 KINEMATIC ANALYSIS	34
4.1 ANGULAR VELOCITIES OF LINKS.....	34
4.2 ANGULAR ACCELERATIONS OF LINKS	37
4.3 VELOCITIES AND ACCELERATIONS OF THE MASS CENTERS OF LINKS.....	41
4.4 SUMMARY.....	44
CHAPTER 5 FORCE ANALYSIS.....	45
5.1 FORCE ANALYSIS.....	45
5.1.1 Static Force Analysis	46
5.1.2 Inertia Force Analysis	52
5.1.3 Complete Result of Force Analysis	56
5.2 MECHANICAL ADVANTAGE.....	60
5.3 SUMMARY.....	61
CHAPTER 6 PERFORMANCE ANALYSIS.....	62
6.1 EVALUATION OF FOOT TRAJECTORY.....	62
6.2 EVALUATION OF MECHANICAL ADVANTAGE	63
6.3 SUMMARY.....	64
CHAPTER 7 PROTOTYPING.....	65
7.1 LAYER ARRANGEMENT FOR LINKS	65
7.2 DETAIL DESIGN OF LINKS AND FAN-SHAPED GEARS.....	69
7.3 COMPUTER SIMULATION.....	72
7.4 PROTOTYPE.....	72
CHAPTER 8 CONCLUSIONS AND SUGGESTIONS.....	75
REFERENCES.....	77
VITA.....	80

自述(VITA in Chinese).....	81
著作權聲明(COPYRIGHT STATEMENT)	82

LIST OF TABLES

Table 3.1	Initial values, lower and upper limits, and optimum values of design variables	29
Table 6.1	Comparison of foot trajectories	63
Table 7.1	Link arrangements for the prototype leg mechanism	68

LIST OF FIGURES

Figure 1.1	Rygg’s patent of a mechanical horse	3
Figure 1.2	Phony Pony	3
Figure 1.3	A quadruped running machine	3
Figure 1.4	Wang’s walking machines.....	4
Figure 1.5	Chen’s wooden horse carriages.....	4
Figure 1.6	Various 8-link type wooden horse carriages	5
Figure 1.7	Chiang’s 10-link type wooden horse carriage.....	5
Figure 1.8	Organization of this thesis	8
Figure 2.1	The amble or walk gait	12
Figure 2.2	The pace gait.....	12
Figure 2.3	The trot gait.....	13
Figure 2.4	The canter gait	13
Figure 2.5	The gallop gait	14
Figure 2.6	The sequence of foot lifting and landing of quadruped creeping gaits.....	14
Figure 2.7	A successive gait pattern of a quadruped with a duty factor of 5/6.....	16
Figure 2.8	A stationary gait pattern of a quadruped with a duty factor of 5/6	16
Figure 2.9	An ideal foot trajectory	17
Figure 3.1	Design flowchart.....	19
Figure 3.2	The leg mechanism of Chiang’s walking machine and its foot trajectory.....	21
Figure 3.3	The coordinate system of the leg mechanism of Chiang’s walking horse.....	22
Figure 3.4	The leg configuration and its foot trajectory after optimization	28
Figure 3.5	A feasible leg mechanism with a duty factor of 0.8.....	31
Figure 3.6	Foot positions of the four legs at the time period $t = 0.2T$	32
Figure 4.1	Position vectors of mass centers relative to the specific pivots.....	43
Figure 5.1	The gait diagram of the designed walking machine with the duty factor of 0.8	45
Figure 5.2	External loads on the walking machine	47
Figure 5.3	Free body diagram of each moving link	48
Figure 5.4	Kinetic diagram of each moving link	49
Figure 5.5	The results of static force analysis of the four legs.....	53

Figure 5.6	The results of inertia force analysis of the four legs.....	57
Figure 5.7	The complete results of force analysis of the four legs	58
Figure 5.8	Driving torque on motor shaft	59
Figure 5.9	Input/output relation for definition of mechanical advantage	61
Figure 6.1	Comparison of foot trajectories	62
Figure 6.2	Mechanical advantage of the designed walking machine.....	63
Figure 7.1	Configuration of the leg mechanism.....	66
Figure 7.2	Final layer arrangement for links.....	68
Figure 7.3	Exterior shape of each link	69
Figure 7.4	Drawings for detail designs of gears.....	70
Figure 7.5	Assembly of the designed walking machine.....	71
Figure 7.6	Successive pictures of animation	73
Figure 7.7	Prototype of the designed walking machine	74

Chapter 1

INTRODUCTION

1.1 Features of Walking Machines

For a long period, human beings have used the wheeled vehicles on paved roads and naturally-flat tracks for fast transportation of great efficiency. However, in natural, a great majority of paths and terrains are not suitable for conventional wheeled vehicles to move on except several particular kinds of vehicles because these natural landforms are rough and uneven, or filled with obstacles and chasms. But for most of the animals living on the land, there are few problems to travel around on these landforms from one place to another on their feet. Therefore, there must be excellent advantages by walking on feet for animals. At certain particular aspects, mankind desires to develop legged vehicles with priority to wheeled ones to do what the wheeled ones are unable to do. And, the legged vehicles are being focused on and used with more and more increasing frequency to take the jobs that are dangerous, in hazardous environment, or on an unknown terrain for humans.

A walking machine or a legged vehicle, as implied in the name, is a machine whose leg mechanisms make itself travel around everywhere on feet or by legs. As a result, it has a great different feature from the common wheeled vehicle that moves on feet which contacts the ground during one part of a period of locomotion and transfers in the air during the other part of that period of locomotion. These two parts are related to “finite states.”

It is summarily said that, in several aspects, there are advantages which make the legged vehicle superior to wheeled ones. As far as mobility is concerned, a walking machine or a legged vehicle is able to walk on a specific terrain or on a variety of landforms on which may be full of obstacles, ramps, chasms, or ditches. With regard to speed, legged vehicles move at faster speed and veer around more easily on rough landforms than conventional wheeled vehicles do, especially on unpaved roads. And,

about energy consumption, walking machines waste less energy since they could adjust the lengths of legs to minimize the undulation of bodies.

In spite that many characteristics of legged vehicles are prior to those of wheeled vehicles, the legged vehicles could not substitute completely for the wheeled vehicles since there are still many difficulties and economic considerations for development of legged vehicles. The developments and researches about legged vehicles are executed in order to displace the tasks which are difficult for the wheeled vehicles or assist the wheeled vehicles in occasions where the wheeled ones and the humans are unable to or have problems to works on. Consequently, to develop legged vehicles owning both the advantages of the legged vehicles and those of the wheeled ones is the main point and has great improvement for our future life.

1.2 Literature Survey

According to the literature regarding the quadruped walking machines [1], Rygg's [2] mechanical horse, Fig. 1.1, constructed by linkages and gears and driven by manpower is the first patent of walking machines. At this stage, the considerations of the design of walking machines were merely on the aspects of leg mechanisms and foot trajectories. However, there is no real mechanical horse to prove the stable walking of his design. In 1960, Shigley [3] proposed several leg mechanisms including four-bar linkages and pantograph mechanisms and built a walking machine with four legs. Moreover, the gait aspect is considered and the gait of his walking machine is controlled by a set of double-rocker mechanisms. In the middle of 20th century, McGhee and Frank [4] created the first computer-controlled walking machine, Phoney Pony, Fig. 1.2. And, later on, the applications of control theories are widely used to design the walking machines such as the walking machine by Hirose [5] and the Running Machine by Raibett [6], Fig. 1.3.

In the past decades although, most of the walking machines were created popularly by the techniques of servo-control, there were scholars and researchers who focused on the designs of walking machines with merely simple mechanisms. In 1986, the "Wooden Ox and Gliding Horse (木牛流馬)," Fig. 1.4(a), which was constructed by two sets of leg mechanisms of 17-bar linkage and pushed forward by manpower was rebuilt by Wang Chien (王湔) [7]. And, moreover in 1992, Wang reconstructed the Lu Ban's (魯班)

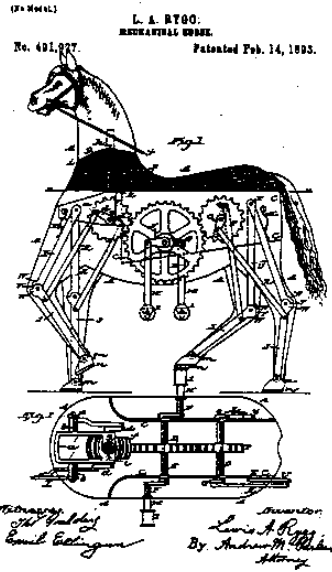


Figure 1.1 Rygg's patent of a mechanical horse [2]

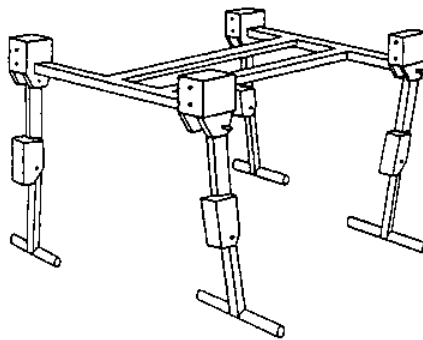


Figure 1.2 Phony Pony [4]

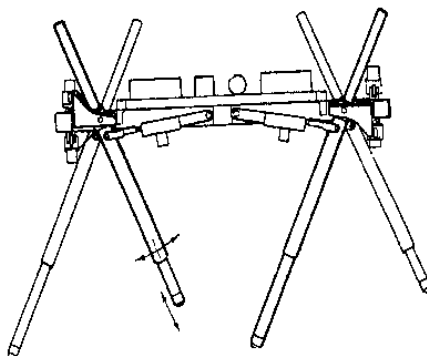


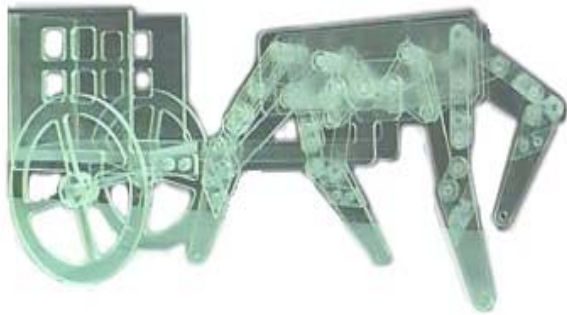
Figure 1.3 A quadruped running machine [6]



(a) Chiu's [10]



(b) Hwang's [11]



(c) Shen's [12]



(d) Hung's [13]

Figure 1.6 Various 8-link type wooden horse carriages



Figure 1.7 Chiang's 10-link type wooden horse carriage [14]

1.3 Motivations and Objectives

In the past years, the reconstructive designs of the walking machines of ancient China by Yan at National Cheng-Kung University (Taiwan, R.O.C.) are powered by man-pushing and are kept their balance with carriages or by man-handling. Recently, questions arise from that when the carriages are dismantled or without man-handling, these walking machines always fall down. How to maintain balance by themselves without the help of carriages or men motivates this research. Furthermore, as far as the economical and uncomplicated aspects are concerned, we would not like to use the expensive and complex controllers and actuators to keep themselves balance. Without the wheeled carriage, the walking machines will not be encumbered with the carriages when they walk on rough terrain and cross obstacles. The main objective of this work is to completely design a walking machine with the leg mechanism of 10-bar linkage and a motor as the power source. And, the walking machine in this work possesses the walking behavior like the mammals, such as horses, oxen, goats, etc. This walking machine uses the specific gait of mammal locomotion to achieve the purpose of balance.

1.4 Organization of Thesis

The organization of this thesis is shown in Fig. 1.8. It is composed of eight chapters. In chapter 1, an introduction to this thesis is presented including the features of walking machines, literature survey, motivations and objectives, and the overall thesis organization. At the beginning of chapter 2, the definitions about walking machines for gait analysis and stability analysis is illustrated. And, what follows are the gait analysis, foot trajectory analysis, and stability analysis. A step-by-step approach to design the self-balanced quadruped walking machine with leg mechanism of 10-bar linkage is addressed about in chapter 3. The kinematic analysis and force analysis including mechanical advantage analysis for the designed walking machine follow in chapters 4 and 5, respectively. After the formulation of analysis is completed, the computer simulation of performance analysis with several comparisons between Chiang's walking machine and the proposed design is performed in chapter 6. Then, in order to verify the feasibility of the designed walking machine, a prototype with the size of Chiang's prototype as reference is constructed and

discussed in chapter 7. Finally in chapter 8, several conclusions are made for this work, and some suggestions are provided for future works.

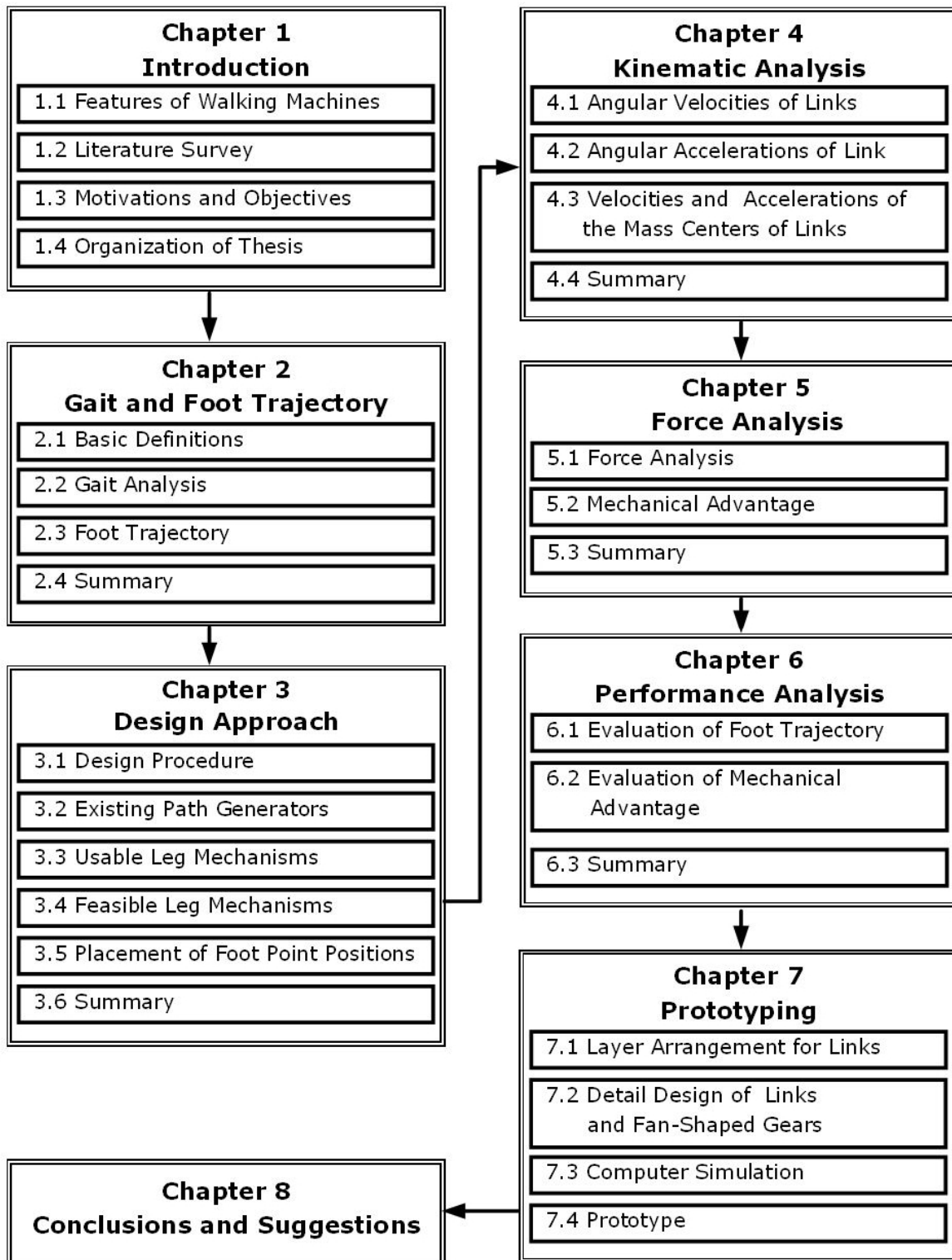


Figure 1.8 Organization of this thesis

Chapter 2

Gait and Foot Trajectory

For legged vehicles, the stability, mobility, adaptive ability, and the speed of locomotion are shown by the gaits and foot trajectories. The study of gaits plays an important role on investigating the characteristics of legged vehicles. The gaits of quadruped animals and the manners to gait analysis are illustrated in this chapter. And, the ideal trajectory for a quadruped walking machine is discussed as well.

2.1 Basic Definitions

At first, the technical terminology for gait study of legged walking machines is defined [15 ~ 17].

- Def. 1: The finite state of the motion of a leg is regarded as two states either on the ground, where the state is 0, or in the air, where the state is 1.
- Def. 2: The leg phase, ϕ_i , of the leg i is the time period having passed by which the leg i is landed on the ground since the landing of leg 1.
- Def. 3: The support phase is the time period at which the leg is on the ground.
- Def. 4: The transfer phase, contrary to the support phase, is the time period at which the leg is in the air.
- Def. 5: The stride is the distance at which a leg moves and recovers to its original configuration related to the body (frame) during a complete cycle of locomotion. It is the same as the distance through which the center of gravity of the body passes in a cycle of locomotion.
- Def. 6: The stroke, R , is the distance by which the foot point moves relative to the body during the support phase.
- Def. 7: The pitch, P , is the center distance between two adjacent strides.
- Def. 8: The relative phase, ϕ_{ij} , is the phase of leg i relative to that of leg j , and is the

time phase having passed by which the leg i is landed on the ground since the landing of leg j . The relative phase is expressed as follows:

$$\phi_{ij} = F(\phi_i - \phi_j) = 1 - \phi_{ji} \quad (2.1)$$

Def. 9: The local phase, ψ_i , of leg i at the current position is the time phase having passed by after the landing of itself. The local phase is expressed as follows:

$$\psi_i = F(t - \phi_{ij}) \quad (2.2)$$

Def. 10: The cycle time is the time period by which the body moves in a complete cycle.

Def. 11: The duty factor, β , is the time period of the support phase during a cycle of locomotion.

Def. 12: The support boundary is the shape on a surface that is formed by the contact points of the feet as the vertices.

Def. 13: The support pattern is the shape on the level ground that is projected from the support boundary.

Def. 14: The stability margin, SM , is the shortest distance from the projection of the center of gravity of the body to the edges of support pattern.

Def. 15: The longitudinal stability margin, LSM , is the shortest distance from the projection of the center of gravity of the body to the edges of the support pattern measured in the longitudinal direction.

Def. 16: The fractional function, $F(x)$, is defined as:

$$\text{If } x \geq 0, \text{ then } F(x) = \text{the fraction part of } x. \quad (2.3a)$$

$$\text{If } x < 0, \text{ then } F(x) = 1 - \text{the fraction part of } (-x). \quad (2.3b)$$

and,

$$F(F(x)) = F(x)$$

$$F(-x) = 1 - F(x)$$

$$F(N + x) = F(M + x), \text{ } N \text{ and } M \text{ are integers.}$$

$$F(A + F(B)) = F(A + B)$$

Def. 17: A regular gait is a gait whose duty factors of all legs are the same.

Def. 18: A symmetric gait is a gait which has a time phase difference of half-period by which the pair of legs at the right-side lands after the pair of legs at the left-side. Otherwise, it is a non-symmetric gait.

Def. 19: A singular gait is if two or more events of support or transfer of legs occur at the same time during the locomotion. Otherwise, it is a non-singular gait.

Def. 20: A walking machine is statically stable if there are at least three legs on the ground and the center of gravity of the body is projected onto the support pattern through the full cycle of locomotion. Otherwise, it is statically unstable.

2.2 Gait Analysis

A gait is the lifting and landing sequences of the legs of an animal and the relationship between the legs when an articulated animal travels around. The study of gaits helps us to understand the walking characteristics of animals. Therefore, the analysis and the use of the gait have great inferences on the stability and the balancing of locomotion of a legged vehicle without numerous actuators and complicated control technology. Here, the common gaits of the quadruped animals and the methods for gait analysis are illustrated in this section.

2.2.1 Gaits of Quadruped Animals

The scientific study of legged locomotion began in the late 19th century. At that time, Muybridge [18] was commissioned to find out whether or not a trotting horse left the ground with all four feet at the same time. He proved this by a set of stop-motion photographs and later, by graphic methods. In modern times, the study of gaits of living things, especially quadruped animals and insects, have applied the graphic methods.

The common-adopted gaits of quadrupeds are classified into five types, amble or walk, trot, canter, pace, and gallop. The detailed descriptions are as follows.

1. Amble or walk (漫步)

The amble or walk is, generally, a slow and four-beat gait as shown in Fig. 2.1(a) [19], and the feet are lifted off the ground in the sequence of left front, right rear, right front, left

rear, separately. Fig. 2.1(b) [20] shows the relative phases of the four legs, where 1, 2, 3, and 4 are the leg numbers. Leg 1 has the relative phase 0 and the others have the relative phases in the range 0 ~ 1.

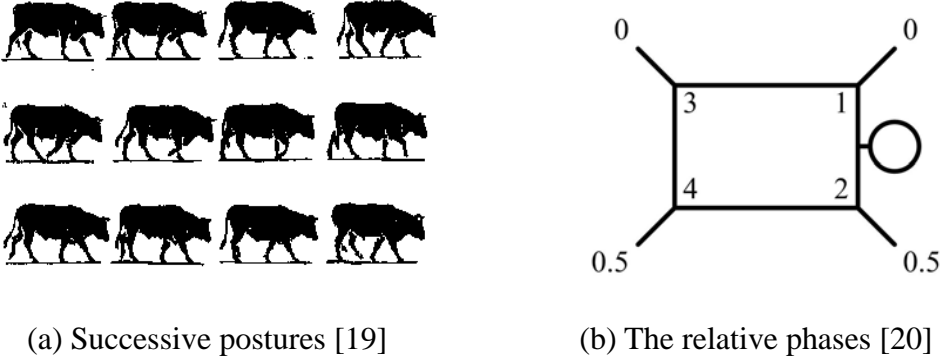


Figure 2.1 The amble or walk gait

2. Pace (溜蹄)

The pace is a fast and laterally two-beat gait with the lateral front and rear legs moving forward and backward together, Fig. 2.2(a) [21]. Therefore, the left two and right two legs are of half-phase difference, Fig. 2.2(b). This kind of gait is adapted by camels.

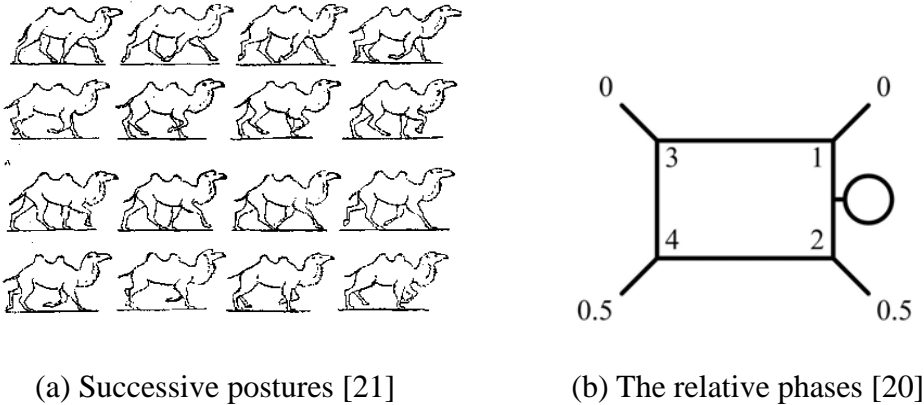


Figure 2.2 The pace gait

3. Trot (疾走)

The trot is a fast and diagonally two-beat gait with the diagonal front and rear legs moving forward and backward together, Fig. 2.3(a) [22]. Therefore, the diagonal legs are of zero-phase difference and the lateral legs are of half-phase difference, Fig. 2.3(b).

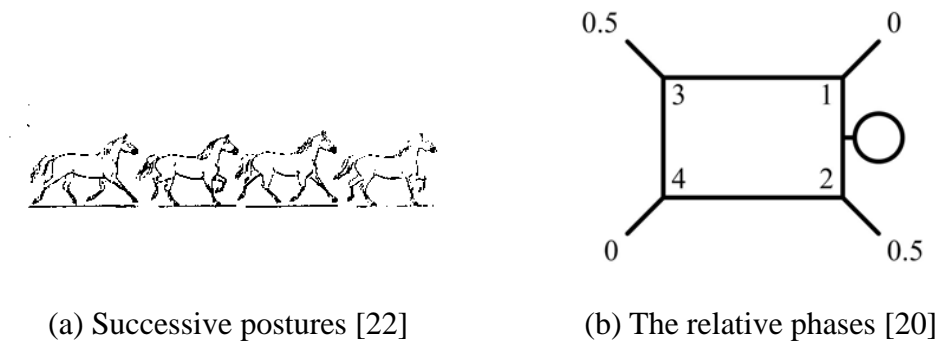


Figure 2.3 The trot gait

4. Canter (小跑)

The canter is a slow, smooth, and straightly three-beat gait, Fig. 2.4(a) [22]. The left front and the right rear legs are of zero-phase difference, and the right front and left rear legs are of about half-phase difference, Fig. 2.4(b). It is a transitional gait between slow and faster gaits.

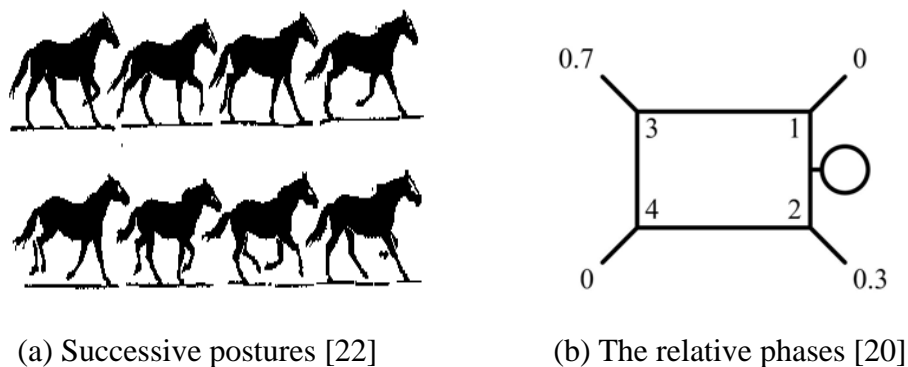


Figure 2.4 The canter gait

5. Gallop (疾馳)

The gallop is a fast and diagonally four-beat gait, Fig. 2.5(a) [23]. The front and the rear legs are of about half-phase difference, and the left and right legs are of slight phase difference. Therefore, the four legs are, simultaneously, in the air at some moments, Fig. 2.5(b).

Besides, there are gaits adopted by animals while they hop, such as the bound (彈跳) gait and the pronk (撲跳) gait. The former is a gait that the front two legs are of zero-phase difference and so are the rear two legs, and the two front legs are of

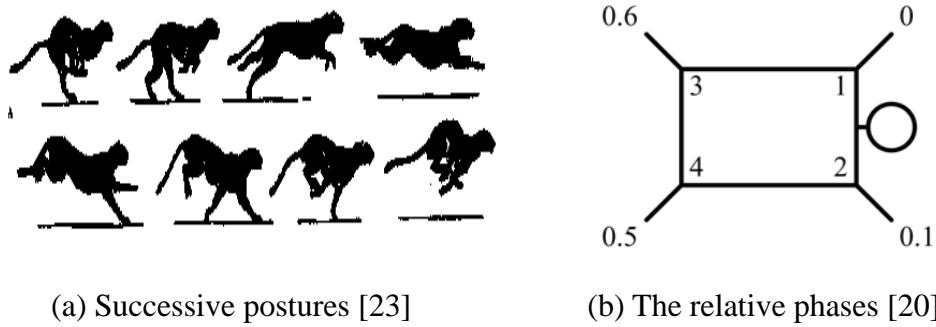


Figure 2.5 The gallop gait

half-difference with the rear two. The latter is a gait with the four legs of zero-phase difference.

It is easy for the living animals to adopt various types of gaits on different terrains to balance themselves. However, it is such a difficult behavior for a walking machine with a unique type of gait to get with various types of terrains. Therefore, amble or walk is a popular type of gait for most quadruped walking machines due to easy balancing. It is proposed by McGhee and Frank [17] that there are three non-singular quadruped gaits by which the walking machines walk in statically stable mode all the time as shown in Fig. 2.6. Among the three gaits, the gait shown in Fig. 2.6(b) is the gait with the optimal static-stability and known as the wave gait adopted by a variety of animals at slow locomotion. And, it is also applied in this study regarding the design of a quadruped walking machine.

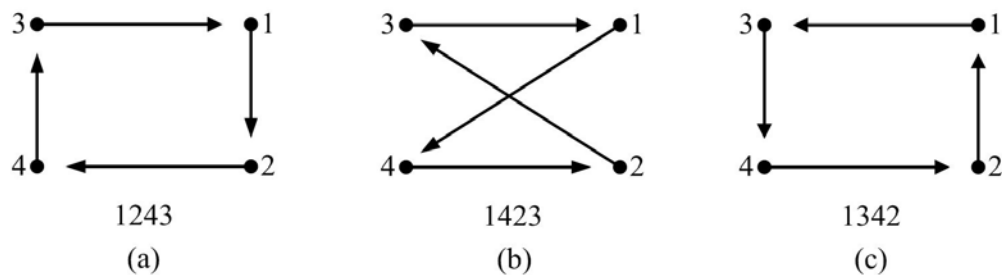


Figure 2.6 The sequence of foot lifting and landing of quadruped creeping gaits [17]

2.2.2 Graphic Methods of Gait Analysis

In order to analyze the gaits, the graphic methods are utilized and described in the

following paragraphs. The successive gait pattern shows the successive support patterns for a gait, and Fig. 2.7 is an example of the successive gait pattern of the wave gait with a duty factor of 5/6. Here, the dotted rectangle is represented the body of the walking machine at a time period with respect to the support pattern. The filled black circles locate the relative positions of the feet on the ground and the hollow circles mean the relative positions of the feet in the air. The black-filled circles with arrows inside the dotted rectangle refer to the positions of the centers of gravity and the directions of motion. The support patterns at different time periods are revealed obviously by these graphs. The longitudinal stability margin is measured and calculated directly from Fig. 2.7. In addition, the stationary gait pattern which is the combination of the successive gait patterns at different time periods is used [15]. By overlapping the dotted rectangles of bodies, Fig. 2.8, in which the symbol, R , indicates the leg stroke and the black-filled circle inside the dotted rectangle means the center of gravity, shows an example of the stationary gait pattern of the wave gait shown in Fig. 2.7. The longitudinal stability margin is directly revealed.

2.3 Foot Trajectory

A foot trajectory is the locus through which the foot point of a leg of a walking machine passes in one cycle of locomotion. It has great influence on the stability of locomotion and adaptive ability to the terrains. In common, a foot trajectory is divided into two portions, support phase and transfer phase. The former is the portion formed when the foot point is in contact with the ground and shown as a straight line-segment in Fig. 2.9. And, the latter is the portion formed when the foot point is in the air. For a quadruped walking machine to achieve statically stable, the time period during support phase relative to the full cycle time must be equal to or greater than 0.75. An ideal foot trajectory should have the characteristics described as follows:

1. The foot trajectory is a closed curve without any intersection.
2. The curve includes a portion of a straight line-segment at the bottom relative to the upper body in order to maintain stability of locomotion during support phase and to reduce oscillation and undulation of the center of gravity of the body.
3. The height of stride is as high as possible to enhance the ability of obstacle-crossing.

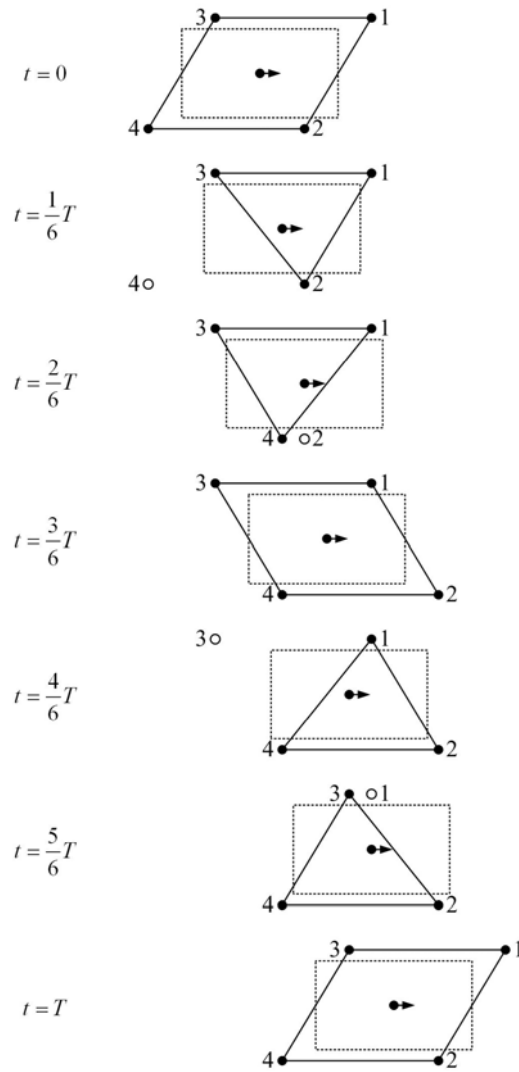


Figure 2.7 A successive gait pattern of a quadruped with a duty factor of 5/6 [15]

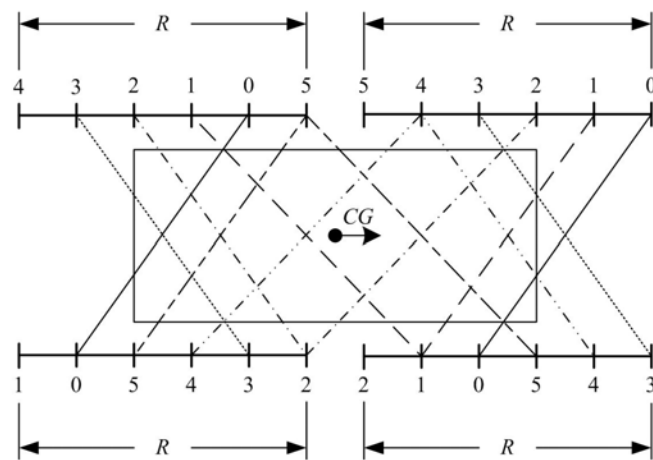


Figure 2.8 A stationary gait pattern of a quadruped with a duty factor of 5/6 [15]

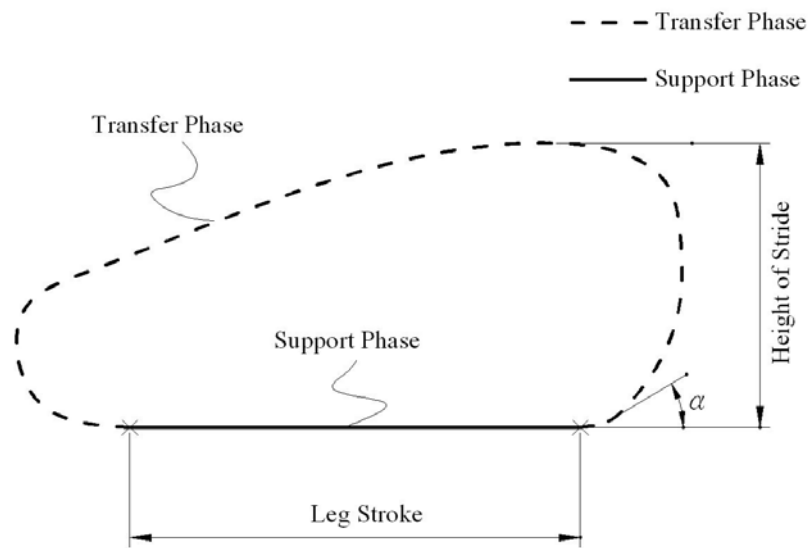


Figure 2.9 An ideal foot trajectory

4. The leg stroke is as long as possible to increase the advancing distance in a stride.
5. The angle α between the ground and the tangent of the end of transfer phase before the foot point enters the support phase is as small as possible to reduce the shock to the leg.

To attain an optimal foot trajectory is the objective of the dimensional synthesis for the leg mechanism in this study.

2.4 Summary

The graphic methods for gait analyses are discussed in this chapter. It provides a quick and useful understanding of the gaits. Besides, in this chapter, the ideal trajectory for the locomotion of a walking machine is mentioned. In the following chapters, the ideal trajectory is targeted as the objective goal for the walking machine.

Chapter 3

Design Approach

In this chapter, a new self-balanced quadruped walking machine with the leg mechanism of 10-bar linkage is systematically designed by a step-by-step approach [24]. The new designed walking machine is expected to achieve statically stable locomotion at a wave gait by the input crank of two speed segments.

3.1 Design Procedure

The flowchart of the design approach proposed by Chen [24] with modification to construct a self-balanced quadruped walking machine with a single actuator is shown in Fig. 3.1. And, the steps for the proposed approach are illustrated as follows. The first step is to investigate and to evaluate existing path generators according to design requirements and constraints. Then, a qualified path generator is chosen as the beginning leg mechanism for dimensional synthesis based on the optimal design techniques. New path generators can be acquired on the basis of Yan's creative mechanism design methodology [8]. The second step is to synthesize the path generator chosen or acquired from the first step to obtain a usable leg mechanism by the techniques of optimal design. A usable leg mechanism is a path generator whose coupler point figures a closed locus with a partially approximate-straight line-segment. Third, the two-speed control method is put into use on the crank of the usable leg mechanism in order to obtain the feasible leg mechanism with sufficient duty factor. The final step is to place the foot point on the right position of the locus at the specific time period based on the gait theory. After the power source and the driving system are installed on the walking machine, the quadruped walking machine is constructed completely. In the following sections of this chapter, the detail design procedure of each step is described.

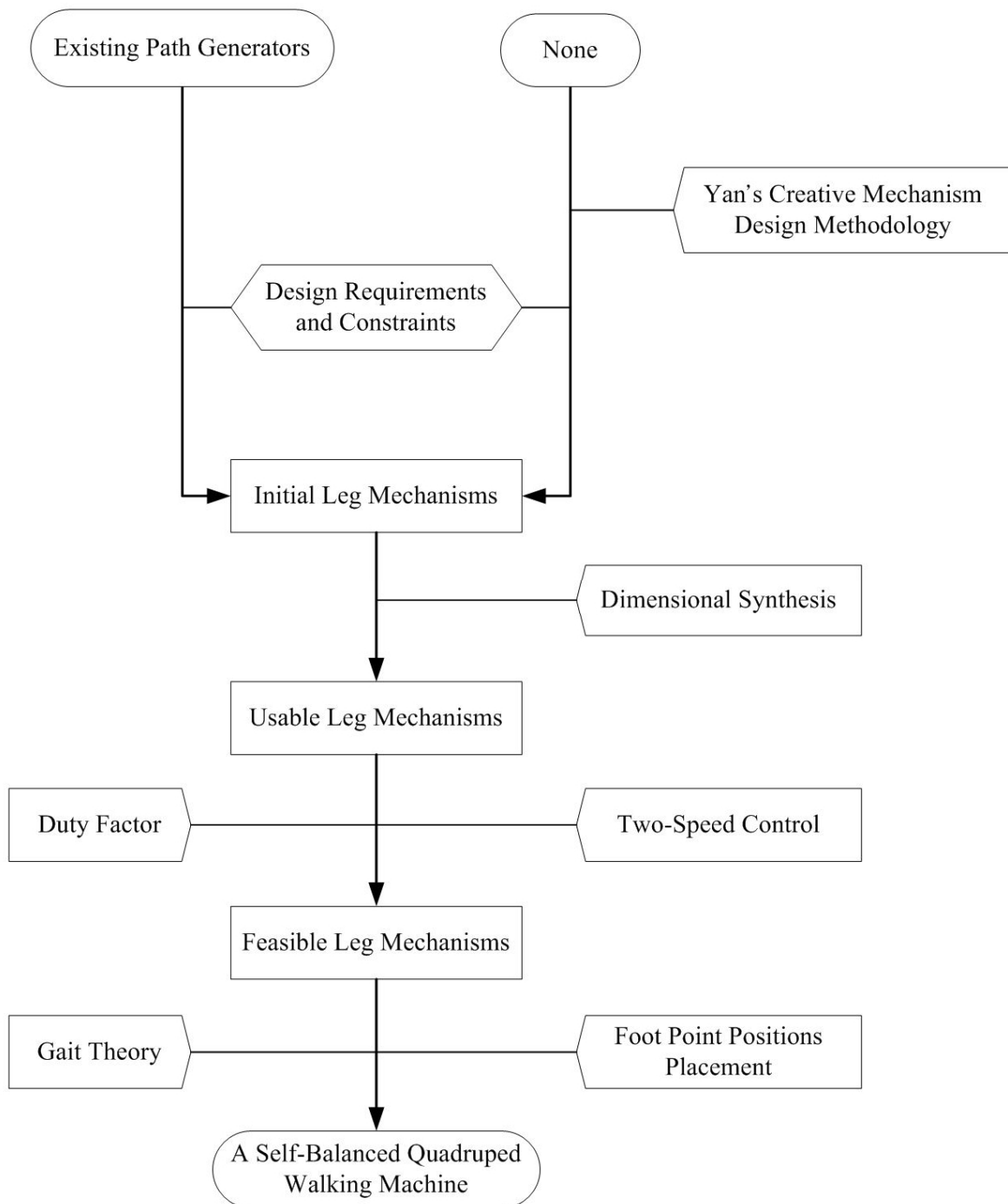


Figure 3.1 Design flowchart

3.2 Existing Path Generators

The first step to design a self-balanced quadruped walking machine is to choose an existing path generator or to synthesize a new one as the initial leg mechanism for usable leg mechanism according to the design constraints and requirements. By these design requirements and constraints, we could check whether the existing path generator conforms to the demands of a leg mechanism for a quadruped walking machine. Or, when developing the new path generators with Yan's creative mechanism design methodology [8], each link of a generalized kinematic chain is assigned for the special purpose by these design requirements and constraints.

To design a mammal type of leg mechanism with 10-bar linkage, the path generator is suggested to satisfy the following requirements and constraints [14]:

1. It is a planar mechanism with one degree-of-freedom.
2. It is a generalized kinematic chain with 10-link and 13-joint. And, in order to reduce the number of candidate generalized kinematic chains, the atlas of kinematic chains with only binary and ternary links are focused.
3. There must be a ground link as the body (frame).
4. The ground link must be a ternary link adjacent to a crank, a femur link, and a connecting link.
5. There must be a crank which is able to rotate a full cycle to generate the successive rotation of motion for the mechanism. And, the crank is a binary link to simplify the structure of the leg mechanism.
6. The crank must be adjacent to the ground link.
7. There must be three individual links as the femur link (股骨桿), the tibia link (脛骨桿), and the cannon link (蹠骨桿) to construct the main structure of the leg, respectively.
8. The femur link must be adjacent to both the ground link and the tibia link.
9. The tibia link must be adjacent to the femur link and the cannon link.
10. The cannon link must be in contact with ground link and adjacent to the tibia link.
11. The tibia link and the cannon link can not be adjacent to the frame.
12. The ground link, the femur link, the tibia link, and the cannon link must be different link.

13. The crank must not be adjacent to any one of the femur, tibia, and cannon links.
14. The femur link is a ternary link adjacent to the ground link, the tibia link, and a connecting link.
15. The tibia link is a ternary link adjacent to the femur link, the cannon link, and a connecting link.
16. The cannon link is a binary link adjacent to the tibia link and a connecting link. And, it should have a coupler point (foot point) to generate the coupler curve without any intersection.
17. All joints incident to links must be revolute joints.

The wooden horse carriage proposed by Chiang, Fig. 1.7, has the leg mechanism with one DOF and with ten links and thirteen revolute joints. The schematic drawing of this leg mechanism and its foot trajectory are shown in Fig. 3.2. Undoubtedly, it meets the design constraints and requirements stated above and it is an existing path generator. By detailed observations, the leg mechanism of this walking machine has a short partial straight line on the foot trajectory and low height of stride. Since this leg mechanism is a 10-bar linkage mechanism, the optimization technique is a suitable way to achieve dimensional synthesis and to obtain a desired foot trajectory.

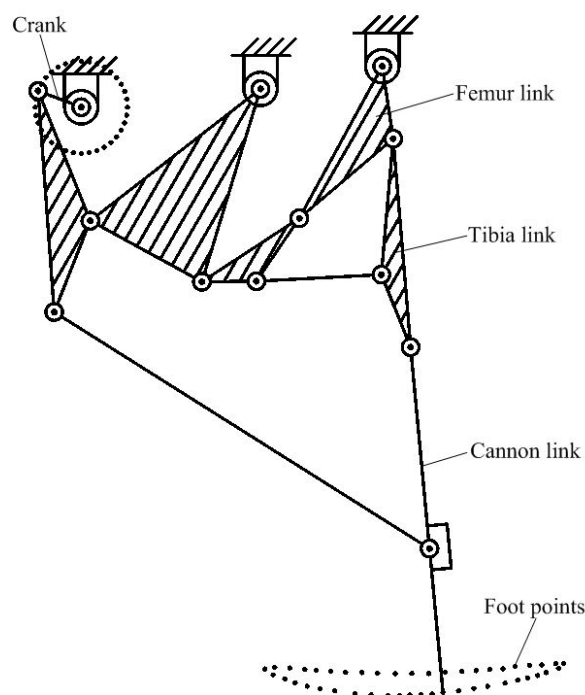


Figure 3.2 The leg mechanism of Chiang's walking machine and its foot trajectory

3.3 Usable Leg Mechanisms

The 10-bar path generator obtained in the previous step is considered not to be a usable leg mechanism until the link dimensions are synthesized and a desired foot trajectory is acquired. Firstly, the equations for position analysis are formulated to recognize the positions of the links and the foot point. And then, the dimensions of links are synthesized by the optimization technique to obtain a usable leg mechanism.

3.3.1 Position Analysis

The coordinate systems on the generalized leg mechanism of Chiang's walking machine are shown in Fig. 3.3 with the vector expressions. Here, XY coordinate is the fixed frame of inertia with the origin O , X_1Y_1 is the coordinate attached to the ground

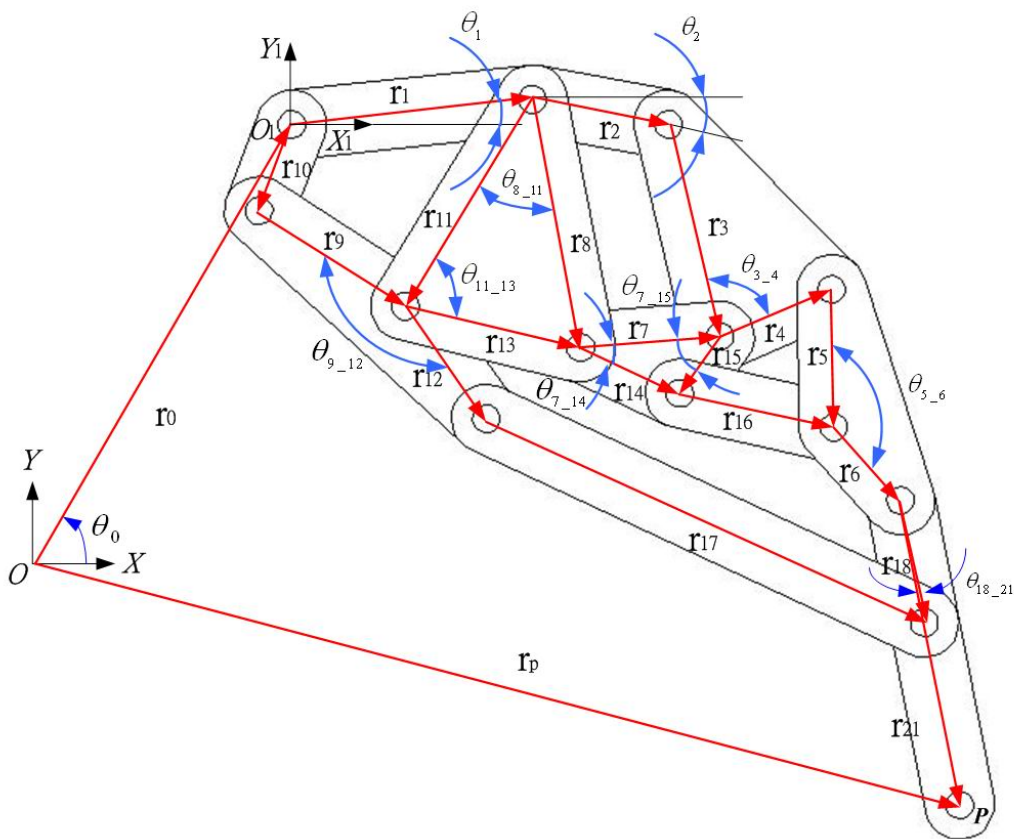


Figure 3.3 The coordinate system of the leg mechanism of Chiang's walking horse

link with origin O_1 , and point P is the foot point of the leg mechanism. Each vector \bar{r} with subscript represents the vector from one joint to another or that from one origin of coordinate system to another, and each angle θ with subscript describes the angle of a vector measured counterclockwise in the positive X axis or the angle between two vectors. A (10, 13) mechanism needs four independent vector loops to determine the positions of all links according to Euler's theory [25] which is:

$$\begin{aligned} L &= J - N + 1 \\ &= 13 - 10 + 1 = 4 \end{aligned}$$

where, L is number of the independent loops, J is the number of simple joints, and N is the number of links. The four independent vector loops are:

$$\text{Loop 1: } \bar{r}_{10} + \bar{r}_{11} - \bar{r}_9 - \bar{r}_1 = 0 \quad (3.1a)$$

$$\text{Loop 2: } \bar{r}_8 + \bar{r}_7 - \bar{r}_3 - \bar{r}_2 = 0 \quad (3.1b)$$

$$\text{Loop 3: } \bar{r}_4 + \bar{r}_5 - \bar{r}_{15} - \bar{r}_{16} = 0 \quad (3.1c)$$

$$\text{Loop 4: } \bar{r}_{13} + \bar{r}_{14} + \bar{r}_{16} + \bar{r}_6 + \bar{r}_{18} - \bar{r}_{12} - \bar{r}_{17} = 0 \quad (3.1d)$$

And, the coordinates of the foot point P of the leg mechanism with respect to XY coordinate is described as:

$$\bar{r}_P = \bar{r}_0 + \bar{r}_1 + \bar{r}_2 + \bar{r}_3 + \bar{r}_4 + \bar{r}_5 + \bar{r}_6 + \bar{r}_{21} \quad (3.2)$$

Eq. (3.1a) is decomposed into the two scale equations as follows:

$$r_{10} \cos \theta_{10} + r_{11} \cos \theta_{11} - r_9 \cos \theta_9 - r_1 \cos \theta_1 = 0 \quad (3.3a)$$

$$r_{10} \sin \theta_{10} + r_{11} \sin \theta_{11} - r_9 \sin \theta_9 - r_1 \sin \theta_1 = 0 \quad (3.3b)$$

where, θ_9 and θ_{11} are unknown variables, θ_1 is a constant, and θ_{10} is the input angle of the crank varying from 0° to 360° . Solving Eqs. (3.3a) and (3.3b) simultaneously, we obtain θ_9 and θ_{11} as follows:

$$\theta_9 = 2 * \tan^{-1}\left(\frac{-b_1 \pm \sqrt{b_1^2 - 4a_1c_1}}{2a_1}\right) \quad (3.3c)$$

$$\theta_{11} = \text{Atan2}(\eta_2 + r_9 \sin \theta_9, \eta_1 + r_9 \cos \theta_9) \quad (3.3d)$$

where

$$\eta_1 = -r_{10} \cos \theta_{10} + r_1 \cos \theta_1$$

$$\eta_2 = -r_{10} \sin \theta_{10} + r_1 \sin \theta_1$$

$$a_1 = r_{11}^2 - \eta_1^2 - \eta_2^2 - r_9^2 + 2r_9\eta_1$$

$$b_1 = -4r_9\eta_2$$

$$c_1 = r_{11}^2 - \eta_1^2 - \eta_2^2 - r_9^2 - 2r_9\eta_1$$

and

$$\theta_8 = \theta_9 + \theta_{9_8}$$

$$\theta_{12} = \theta_{11} + \theta_{11_12}$$

$$\theta_{13} = \theta_9 + \theta_{9_13}$$

In the same manner, Eqs. (3.1b) is decomposed into two scale equations as follows:

$$r_8 \cos \theta_8 + r_7 \cos \theta_7 - r_3 \cos \theta_3 - r_2 \cos \theta_2 = 0 \quad (3.4a)$$

$$r_8 \sin \theta_8 + r_7 \sin \theta_7 - r_3 \sin \theta_3 - r_2 \sin \theta_2 = 0 \quad (3.4b)$$

where, θ_3 and θ_7 are unknown variables, θ_2 is a constant, and θ_8 is provided by loop 1. Solving Eqs. (3.4a) and (3.4b) simultaneously, we have θ_3 and θ_7 , as below:

$$\theta_3 = 2 * \tan^{-1}\left(\frac{-b_2 \pm \sqrt{b_2^2 - 4a_2c_2}}{2a_2}\right) \quad (3.4c)$$

$$\theta_7 = \text{Atan2}(\eta_4 + r_3 \sin \theta_3, \eta_3 + r_3 \cos \theta_3) \quad (3.4d)$$

where

$$\eta_3 = -r_8 \cos \theta_8 + r_2 \cos \theta_2$$

$$\eta_4 = -r_8 \sin \theta_8 + r_2 \sin \theta_2$$

$$a_2 = r_7^2 - \eta_3^2 - \eta_4^2 - r_3^2 + 2r_3\eta_3$$

$$b_2 = -4r_3\eta_4$$

$$c_2 = r_7^2 - \eta_3^2 - \eta_4^2 - r_3^2 - 2r_3\eta_3$$

and

$$\theta_4 = \theta_3 + \theta_{3_4}$$

$$\theta_{15} = \theta_7 + \theta_{7_15}$$

$$\theta_{14} = \theta_7 + \theta_{7_14}$$

In the same manner, Eq. (3.1c) is decomposed into two scale equations as follows:

$$r_4 \cos \theta_4 + r_5 \cos \theta_5 - r_{15} \cos \theta_{15} - r_{16} \cos \theta_{16} = 0 \quad (3.5a)$$

$$r_4 \sin \theta_4 + r_5 \sin \theta_5 - r_{15} \sin \theta_{15} - r_{16} \sin \theta_{16} = 0 \quad (3.5b)$$

where θ_5 and θ_{16} are unknown variables, θ_4 and θ_{15} are provided by loop 2.

Solving the Eqs. (3.5a) and (3.5b) simultaneously, we obtain θ_5 and θ_{16} , as follows:

$$\theta_5 = 2 * \tan^{-1} \left(\frac{-b_3 \pm \sqrt{b_3^2 - 4a_3c_3}}{2a_3} \right) \quad (3.5c)$$

$$\theta_{16} = \text{Atan2}(\eta_6 + r_5 \sin \theta_5, \eta_5 + r_5 \cos \theta_5) \quad (3.5d)$$

where

$$\eta_5 = -r_{15} \cos \theta_{15} + r_4 \cos \theta_4$$

$$\eta_6 = -r_{15} \sin \theta_{15} + r_4 \sin \theta_4$$

$$a_3 = r_{16}^2 - \eta_5^2 - \eta_6^2 - r_5^2 + 2r_5\eta_5$$

$$b_3 = -4r_5\eta_6$$

$$c_3 = r_{16}^2 - \eta_5^2 - \eta_6^2 - r_5^2 - 2r_5\eta_5$$

and

$$\theta_6 = \theta_5 + \theta_{5_6}$$

In the same manner, Eq. (3.1d) is decomposed into two scale equations as follows:

$$\begin{aligned} r_{13} \cos \theta_{13} + r_{14} \cos \theta_{14} \\ + r_{16} \cos \theta_{16} + r_6 \cos \theta_6 + r_{18} \cos \theta_{18} - r_{12} \cos \theta_{12} - r_{17} \cos \theta_{17} = 0 \end{aligned} \quad (3.6a)$$

$$\begin{aligned} r_{13} \sin \theta_{13} + r_{14} \sin \theta_{14} \\ + r_{16} \sin \theta_{16} + r_6 \sin \theta_6 + r_{18} \sin \theta_{18} - r_{12} \sin \theta_{12} - r_{17} \sin \theta_{17} = 0 \end{aligned} \quad (3.6b)$$

where θ_{17} and θ_{18} are unknown variables, and θ_{13} , θ_{14} , θ_{16} , θ_6 , and θ_{12} are provided by loop 1~3. Solving the Eqs. (3.6a) and (3.6b) simultaneously, we have θ_{17} and θ_{18} , as follows:

$$\theta_{18} = 2 * \tan^{-1} \left(\frac{-b_4 \pm \sqrt{b_4^2 - 4a_4c_4}}{2a_4} \right) \quad (3.6c)$$

$$\theta_{17} = \text{Atan2}(\eta_8 + r_{18} \sin \theta_{18}, \eta_7 + r_{18} \cos \theta_{18}) \quad (3.6d)$$

where

$$\eta_7 = r_{13} \cos \theta_{13} + r_{14} \cos \theta_{14} + r_{16} \cos \theta_{16} + r_6 \cos \theta_6 - r_{12} \cos \theta_{12}$$

$$\eta_8 = r_{13} \sin \theta_{13} + r_{14} \sin \theta_{14} + r_{16} \sin \theta_{16} + r_6 \sin \theta_6 - r_{12} \sin \theta_{12}$$

$$a_4 = r_{17}^2 - \eta_7^2 - \eta_8^2 - r_{18}^2 + 2r_{18}\eta_7$$

$$b_4 = -4r_{18}\eta_8$$

$$c_4 = r_{17}^2 - \eta_7^2 - \eta_8^2 - r_{18}^2 - 2r_{18}\eta_7$$

and

$$\theta_{21} = \theta_{18} + \theta_{18_21}$$

3.3.2 Dimensional Synthesis

The 10-link path generator in Fig. 3.3 needs to be iteratively performed dimensional synthesis to obtain a usable leg mechanism with the desired foot trajectory. The design variables are the lengths of vectors (r_0 , r_1 , r_2 , r_3 , r_4 , r_5 , r_6 , r_7 , r_8 , r_9 , r_{10} , r_{11} , r_{12} , r_{15} , r_{16} , r_{17} , r_{18} , and r_{21}), the orientations of vectors (θ_0 , θ_1 , and θ_2), the angles between two vectors (θ_{3_4} , θ_{5_6} , θ_{7_15} , θ_{9_8} , θ_{11_12} , and θ_{18_21}), and n prescribed positions of the input crank ($\theta_{10_1} \sim \theta_{10_n}$). The foot trajectory of the leg mechanism is

desired to pass through the n specified positions, $P_1 \sim P_n$, with n prescribed positions of input crank ($\theta_{10,1} \sim \theta_{10,n}$). Here, five specified positions are desired to be passed through, and therefore, there are 32 design variables in the optimization problem. The objective function is formulated as follows:

$$\text{Min. } F(\bar{r}_1) = w_1 \sum_{i=1}^5 (x_i - x_{si})^2 + w_2 \sum_{i=1}^5 (y_i - y_{si})^2 \quad (3.7)$$

where x_{si} and y_{si} are x and y components of the i -th specified positions, x_i and y_i are x and y components of the actual positions of foot points at the prescribed angles of input crank, and w_1 and w_2 are the weighting factors. And, the inequality design constraints to confirm that loop 1 is a crank-rocker mechanism is as follows:

$$g_1(x) = r_1 - r_9 + r_{10} - r_{11} \leq 0 \quad (3.8a)$$

$$g_2(x) = r_9 - r_1 + r_{10} - r_{11} \leq 0 \quad (3.8b)$$

$$g_3(x) = r_{10} - r_1 - r_9 + r_{11} \leq 0 \quad (3.8c)$$

In order to decrease the number of design variables, the length of vector \bar{r}_1 is set to be unity and $\theta_{18,21}$ is set to be 0. And, the leg mechanism is desired to have the length of a partial straight line-segment of 1, and to have a height of stride of 0.6. The five specified positions on the desired foot trajectory are $P_1(2.0, -2.5)$, $P_2(1.5, -2.5)$, $P_3(1.0, -2.5)$, $P_4(1.25, -1.9)$, and $P_5(1.75, -1.9)$, as shown in Fig. 3.4. Besides, both of the weighting factors, w_1 and w_2 , are 0.5. Therefore, there are 31 design variables, 3 inequality constraints in this optimization problem. The initial values, lower and upper bounds, and the optimum values of design variables by the augmented Lagrange multiplier method [26] are listed in Table 3.1.

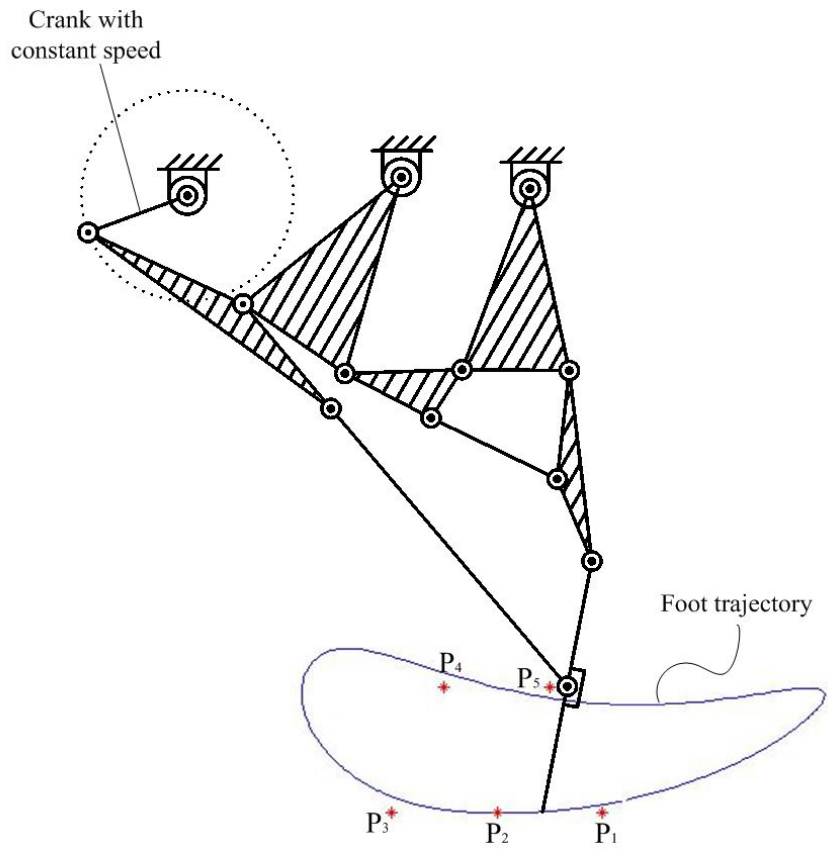


Figure 3.4 The leg configuration and its foot trajectory after optimization

Table 3.1 Initial values, lower and upper limits, and optimum values of design variables

Design Variables	r_0 (mm)	r_1 (mm)	r_2 (mm)	r_3 (mm)	r_4 (mm)	r_5 (mm)	r_6 (mm)	r_7 (mm)	r_8 (mm)	r_9 (mm)	r_{10} (mm)
Initial Values	1	/	0.6832	0.9635	0.6781	0.7487	0.4467	0.6463	1.1202	1.1925	0.2508
Upper Limits	0.1	/	0.1	0.5	0.3	0.3	0.3	0.2	0.5	0.5	0.1
Lower Limits	5	/	2	1.5	1	1	1	1	1.5	1.5	0.6
Optimum Values	0.0014	1	0.6	0.91	0.5	0.51	0.43	0.55	0.96	0.95	0.5

Design Variables	r_{11} (mm)	r_{12} (mm)	r_{15} (mm)	r_{16} (mm)	r_{17} (mm)	r_{18} (mm)	r_{21} (mm)
Initial Values	0.7689	0.538	0.4221	0.6918	2.21	0.6657	1.8924
Upper Limits	0.2	0.2	0.2	0.3	1.5	0.1	0.1
Lower Limits	0.9	0.9	1	0.8	2.5	0.8	0.8
Optimum Values	0.8	0.65	0.27	0.65	1.7	0.6	1.2

Design Variables	θ_0 (rad)	θ_1 (rad)	θ_2 (rad)	$\theta_{3,4}$ (rad)	$\theta_{5,6}$ (rad)	$\theta_{7,15}$ (rad)	$\theta_{9,8}$ (rad)	$\theta_{11,12}$ (rad)	$\theta_{18,21}$ (rad)
Initial Values	0.7854	0.1047	0.1895	0.3674	2.6934	0.4046	0.6084	2.3735	/
Upper Limits	0	0	0	0	0	0	0	0	/
Lower Limits	3.14	3.14	3.14	3.14	3.14	3.14	3.14	3.14	/
Optimum Values	0.0294	0.0873	-0.0873	1.9199	0.5236	4.1015	0.6109	5.8468	0

Design Variables	$\theta_{10,1}$ (rad)	$\theta_{10,2}$ (rad)	$\theta_{10,3}$ (rad)	$\theta_{10,4}$ (rad)	$\theta_{10,5}$ (rad)
Initial Values	0.5235	1.1345	1.6755	4.1015	5.4978
Upper Limits	0	0	0	0	0
Lower Limits	3.14	3.14	3.14	3.14	3.14
Optimum Values	0.14	2	2.9	4.04	5.9795

Figure 3.4 shows the schematic drawing of the leg mechanism and its corresponding foot trajectory. It is observed that there is an approximately straight line-segment between around the points P_1 and P_3 , and this line-segment is available for the support phase of the leg mechanism. From the computer program and the output diagram, it is realized that when the input crank of the leg mechanism rotates from -227° to -135° clockwise, the foot point moves from around P_1 to around P_3 . As the crank rotates at a constant speed, the duty factor is:

$$\beta = \frac{(227^\circ - 134^\circ)}{360^\circ} \approx 0.26$$

Obviously, it is not sufficient for the statically stable walking.

3.4 Feasible Leg Mechanisms

According to the interval of the high segment, that of low speed segment, and the desired duty factor, the speed ratio is calculated as follows:

$$R_\omega = \frac{\frac{\theta_H}{\theta_S}}{\frac{1}{\beta} - 1} \quad (3.9)$$

where $\theta_S = 93^\circ$, $\theta_L = 93^\circ$, $\theta_H = 360^\circ - \theta_S = 267^\circ$. A β value of 0.8 is desired and therefore, we obtain $R_\omega \approx 11.48$. Fig. 3.5 shows a feasible leg mechanism with the crank whose speed ratio, R_ω , is 11.48.

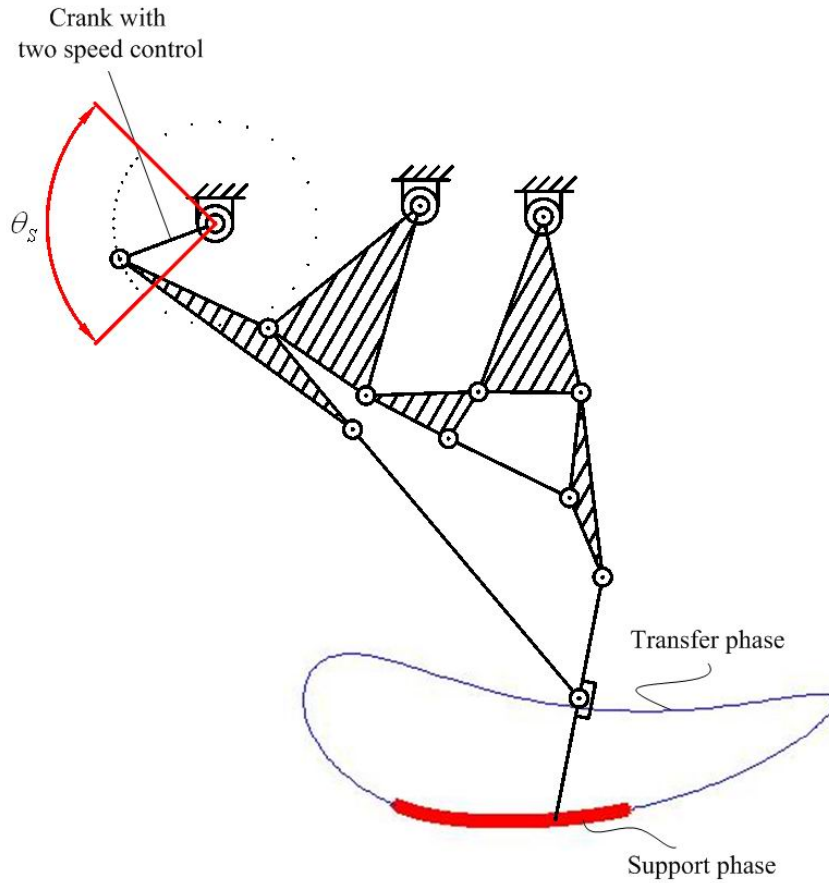


Figure 3.5 A feasible leg mechanism with a duty factor of 0.8

3.5 Placement of Foot-Point Positions

Based on the gait theory, we are able to obtain the relative phase and the local phase of each foot for the wave gait of duty factor 0.8. The relative phases are:

$$\phi_1 = 0$$

$$\phi_2 = 0.5$$

$$\phi_3 = \beta = 0.8$$

$$\phi_4 = F(\beta - 0.5) = 0.3$$

If we take time phase $t = 0.2T$ where T is the period of a full locomotion, the local phases of the four legs are as follows:

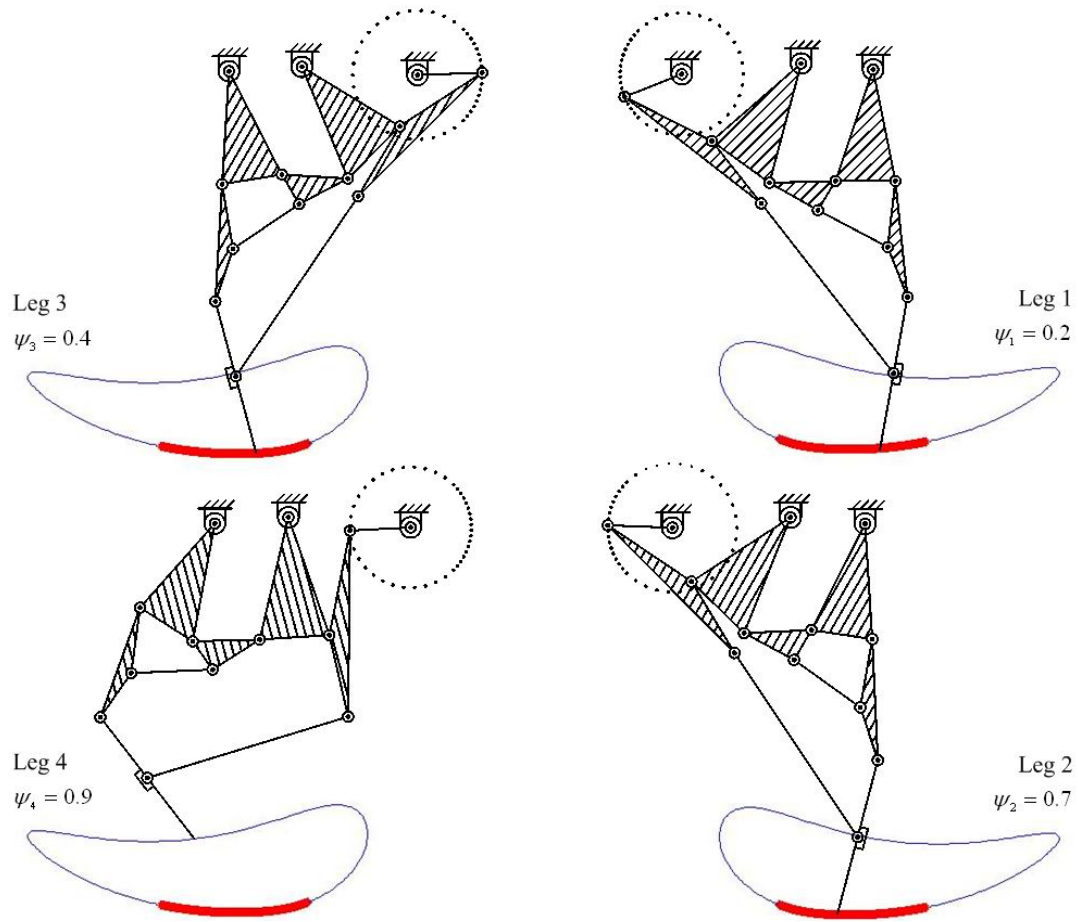


Figure 3.6 Foot positions of the four legs at the time period $t = 0.2T$

$$\psi_1 = F(t - \phi_1) = 0.2$$

$$\psi_2 = F(t - \phi_2) = 0.7$$

$$\psi_3 = F(t - \phi_3) = 0.4$$

$$\psi_4 = F(t - \phi_4) = 0.9$$

The configurations of the four legs at time phase $t = 0.2T$ can be obtained according to the local phases and foot point positions of the four legs as shown in Fig. 3.6. The local phase 0.9 of leg 4 means that leg 4 is at the transfer phase; that is, it is in the air at the time of 0.2.

3.6 Summary

In this chapter, the procedure of designing a self-balanced walking machine with the leg mechanism of 10-bar linkage is illustrated according to the approach described in section 3.2. The leg mechanism of Chiang's wooden horse carriage is chosen as the initial leg mechanism to synthesize a usable leg mechanism and, moreover, a feasible leg mechanism. Based on the leg mechanism obtained in this chapter, we can perform kinematic analysis and force analysis in the next two chapters to obtain the characteristics of the leg mechanism and those of the walking machine.

Chapter 4

Kinematic Analysis

In accordance with the usable leg mechanism developed in Chapter 3, the kinematic analysis is performed in this chapter. Since the position analysis is completed in designing the usable leg mechanism, here we start the kinematic analysis with the velocity analysis according to the results of position analysis.

4.1 Angular Velocities of Links

Differentiating Eqs. (3.3a,b), (3.4a,b), (3.5a,b), and (3.6a,b) of position analyses of the four loops with respect to time, and we can obtain Eqs. (4.1), (4.3), (4.5), and (4.7) for the angular velocities of the nine moving links.

Loop 1

$$-r_{11}\omega_{11} \sin \theta_{11} + r_9\omega_9 \sin \theta_9 = r_{10}\omega_{10} \sin \theta_{10} \quad (4.1a)$$

$$r_{11}\omega_{11} \cos \theta_{11} - r_9\omega_9 \cos \theta_9 = -r_{10}\omega_{10} \cos \theta_{10} \quad (4.1b)$$

where ω_{11} and ω_9 are unknown angular velocities of links 2 and 4, respectively, and ω_{10} is the constant crank speed of link 1. With Cramer's rule, this set of simultaneous equations could be solved, and we have:

$$\omega_{11} = \frac{\Delta_{11}}{\Delta_1} \quad (4.2a)$$

$$\omega_9 = \frac{\Delta_{12}}{\Delta_1} \quad (4.2b)$$

where

$$\Delta_1 = \begin{vmatrix} -r_{11} \sin \theta_{11} & r_9 \sin \theta_9 \\ r_{11} \cos \theta_{11} & -r_9 \cos \theta_9 \end{vmatrix}$$

$$\Delta_{11} = \begin{vmatrix} r_{10} \omega_{10} \sin \theta_{10} & r_9 \sin \theta_9 \\ -r_{10} \omega_{10} \cos \theta_{10} & -r_9 \cos \theta_9 \end{vmatrix}$$

$$\Delta_{12} = \begin{vmatrix} -r_{11} \sin \theta_{11} & r_{10} \omega_{10} \sin \theta_{10} \\ r_{11} \cos \theta_{11} & -r_{10} \omega_{10} \cos \theta_{10} \end{vmatrix}$$

Loop 2

$$-r_7 \omega_7 \sin \theta_7 + r_3 \omega_3 \sin \theta_3 = r_8 \omega_8 \sin \theta_8 \quad (4.3a)$$

$$r_7 \omega_7 \cos \theta_7 - r_3 \omega_3 \cos \theta_3 = -r_8 \omega_8 \cos \theta_8 \quad (4.3b)$$

where ω_7 and ω_3 are unknown angular velocities of links 5 and 7, respectively, and $\omega_8 = \omega_9$ is the angular velocity of link 4 which is obtained after the velocity analysis of loop 1. Similarly, with Cramer's rule, we have:

$$\omega_7 = \frac{\Delta_{21}}{\Delta_2} \quad (4.4a)$$

$$\omega_3 = \frac{\Delta_{22}}{\Delta_2} \quad (4.4b)$$

where

$$\Delta_2 = \begin{vmatrix} -r_7 \sin \theta_7 & r_3 \sin \theta_3 \\ r_7 \cos \theta_7 & -r_3 \cos \theta_3 \end{vmatrix}$$

$$\Delta_{21} = \begin{vmatrix} r_8 \omega_8 \sin \theta_8 & r_3 \sin \theta_3 \\ -r_8 \omega_8 \cos \theta_8 & -r_3 \cos \theta_3 \end{vmatrix}$$

$$\Delta_{22} = \begin{vmatrix} -r_7 \sin \theta_7 & r_8 \omega_8 \sin \theta_8 \\ r_7 \cos \theta_7 & -r_8 \omega_8 \cos \theta_8 \end{vmatrix}$$

Loop 3

$$-r_{16}\omega_{16} \sin \theta_{16} + r_5\omega_5 \sin \theta_5 = -r_4\omega_4 \sin \theta_4 + r_{15}\omega_{15} \sin \theta_{15} \quad (4.5a)$$

$$r_{16}\omega_{16} \cos \theta_{16} - r_5\omega_5 \cos \theta_5 = r_4\omega_4 \cos \theta_4 - r_{15}\omega_{15} \cos \theta_{15} \quad (4.5b)$$

where ω_{16} and ω_5 are unknown angular velocities of links 6 and 8, respectively, and $\omega_4 = \omega_3$ and $\omega_{15} = \omega_7$ are the angular velocities of links 7 and 5. Again, with Cramer's rule, we have:

$$\omega_{16} = \frac{\Delta_{31}}{\Delta_3} \quad (4.6a)$$

$$\omega_5 = \frac{\Delta_{32}}{\Delta_3} \quad (4.6b)$$

where

$$\Delta_3 = \begin{vmatrix} -r_{16} \sin \theta_{16} & r_5 \sin \theta_5 \\ r_{16} \cos \theta_{16} & -r_5 \cos \theta_5 \end{vmatrix}$$

$$\Delta_{31} = \begin{vmatrix} -r_4\omega_4 \sin \theta_4 + r_{15}\omega_{15} \sin \theta_{15} & r_5 \sin \theta_5 \\ r_4\omega_4 \cos \theta_4 - r_{15}\omega_{15} \cos \theta_{15} & -r_5 \cos \theta_5 \end{vmatrix}$$

$$\Delta_{32} = \begin{vmatrix} -r_{16} \sin \theta_{16} & -r_4\omega_4 \sin \theta_4 + r_{15}\omega_{15} \sin \theta_{15} \\ r_{16} \cos \theta_{16} & r_4\omega_4 \cos \theta_4 - r_{15}\omega_{15} \cos \theta_{15} \end{vmatrix}$$

Loop 4

$$\begin{aligned} -r_{17}\omega_{17} \sin \theta_{17} + r_{18}\omega_{18} \sin \theta_{18} &= -r_8\omega_8 \sin \theta_8 + r_9\omega_9 \sin \theta_9 - r_7\omega_7 \sin \theta_7 \\ &\quad - r_{15}\omega_{15} \sin \theta_{15} - r_{16}\omega_{16} \sin \theta_{16} - r_6\omega_6 \sin \theta_6 \\ &\quad + r_{12}\omega_{12} \sin \theta_{12} \end{aligned} \quad (4.7a)$$

$$\begin{aligned} r_{17}\omega_{17} \cos \theta_{17} - r_{18}\omega_{18} \cos \theta_{18} &= r_8\omega_8 \cos \theta_8 - r_9\omega_9 \cos \theta_9 + r_7\omega_7 \cos \theta_7 \\ &\quad + r_{15}\omega_{15} \cos \theta_{15} + r_{16}\omega_{16} \cos \theta_{16} + r_6\omega_6 \cos \theta_6 \\ &\quad - r_{12}\omega_{12} \cos \theta_{12} \end{aligned} \quad (4.7b)$$

where ω_{17} and ω_{18} are unknown angular velocities of links 3 and 9, respectively, and $\omega_6 = \omega_5$ and $\omega_{12} = \omega_{11}$ are the angular velocities of links 8 and 2. Then,

$$\omega_{17} = \frac{\Delta_{41}}{\Delta_4} \quad (4.8a)$$

$$\omega_{18} = \frac{\Delta_{42}}{\Delta_4} \quad (4.8b)$$

where

$$\Delta_4 = \begin{vmatrix} -r_{17} \sin \theta_{17} & r_{18} \sin \theta_{18} \\ r_{17} \cos \theta_{17} & -r_{18} \cos \theta_{18} \end{vmatrix}$$

$$\Delta_{41} = \begin{vmatrix} \left(\begin{array}{c} -r_8 \omega_8 \sin \theta_8 + r_9 \omega_9 \sin \theta_9 - r_7 \omega_7 \sin \theta_7 - r_{15} \omega_{15} \sin \theta_{15} \\ -r_{16} \omega_{16} \sin \theta_{16} - r_6 \omega_6 \sin \theta_6 + r_{12} \omega_{12} \sin \theta_{12} \end{array} \right) & r_{18} \sin \theta_{18} \\ \left(\begin{array}{c} r_8 \omega_8 \cos \theta_8 - r_9 \omega_9 \cos \theta_9 + r_7 \omega_7 \cos \theta_7 + r_{15} \omega_{15} \cos \theta_{15} \\ + r_{16} \omega_{16} \cos \theta_{16} + r_6 \omega_6 \cos \theta_6 - r_{12} \omega_{12} \cos \theta_{12} \end{array} \right) & -r_{18} \cos \theta_{18} \end{vmatrix}$$

$$\Delta_{42} = \begin{vmatrix} -r_{17} \sin \theta_{17} & \left(\begin{array}{c} -r_8 \omega_8 \sin \theta_8 + r_9 \omega_9 \sin \theta_9 - r_7 \omega_7 \sin \theta_7 - r_{15} \omega_{15} \sin \theta_{15} \\ -r_{16} \omega_{16} \sin \theta_{16} - r_6 \omega_6 \sin \theta_6 + r_{12} \omega_{12} \sin \theta_{12} \end{array} \right) \\ r_{17} \cos \theta_{17} & \left(\begin{array}{c} r_8 \omega_8 \cos \theta_8 - r_9 \omega_9 \cos \theta_9 + r_7 \omega_7 \cos \theta_7 + r_{15} \omega_{15} \cos \theta_{15} \\ + r_{16} \omega_{16} \cos \theta_{16} + r_6 \omega_6 \cos \theta_6 - r_{12} \omega_{12} \cos \theta_{12} \end{array} \right) \end{vmatrix}$$

4.2 Angular Accelerations of Links

With the results of angular velocity analysis, the angular acceleration analysis could be performed. Differentiating the equations for angular velocity analysis, Eq. (4.1), (4.3), (4.5), and (4.7), with respect to time, we have the following another four sets of simultaneous equations.

Loop 1

$$-r_{11} \alpha_{11} \sin \theta_{11} + r_9 \alpha_9 \sin \theta_9 = r_{10} \alpha_{10} \sin \theta_{10} + r_{10} \omega_{10}^2 \cos \theta_{10} + r_{11} \omega_{11}^2 \cos \theta_{11} - r_9 \omega_9^2 \cos \theta_9 \quad (4.9a)$$

$$r_{11} \alpha_{11} \cos \theta_{11} - r_9 \alpha_9 \cos \theta_9 = -r_{10} \alpha_{10} \cos \theta_{10} + r_{10} \omega_{10}^2 \sin \theta_{10} + r_{11} \omega_{11}^2 \sin \theta_{11} - r_9 \omega_9^2 \sin \theta_9 \quad (4.9b)$$

where α_{11} and α_9 are unknown angular accelerations of links 2 and 4, respectively, and

α_{10} is angular acceleration of input crank which rotates with constant speed; that is, α_{10} equals to zero. With Cramer's rule, we have:

$$\alpha_{11} = \frac{\Lambda_{11}}{\Lambda_1} \quad (4.10a)$$

$$\alpha_9 = \frac{\Lambda_{12}}{\Lambda_1} \quad (4.10b)$$

where

$$\Lambda_1 = \Delta_1$$

$$\Lambda_{11} = \begin{vmatrix} r_{10}\alpha_{10} \sin \theta_{10} + r_{10}\omega_{10}^2 \cos \theta_{10} + r_{11}\omega_{11}^2 \cos \theta_{11} - r_9\omega_9^2 \cos \theta_9 & r_9 \sin \theta_9 \\ -r_{10}\alpha_{10} \cos \theta_{10} + r_{10}\omega_{10}^2 \sin \theta_{10} + r_{11}\omega_{11}^2 \sin \theta_{11} - r_9\omega_9^2 \sin \theta_9 & -r_9 \cos \theta_9 \end{vmatrix}$$

$$\Lambda_{12} = \begin{vmatrix} -r_{11} \sin \theta_{11} & r_{10}\alpha_{10} \sin \theta_{10} + r_{10}\omega_{10}^2 \cos \theta_{10} + r_{11}\omega_{11}^2 \cos \theta_{11} - r_9\omega_9^2 \cos \theta_9 \\ r_{11} \cos \theta_{11} & -r_{10}\alpha_{10} \cos \theta_{10} + r_{10}\omega_{10}^2 \sin \theta_{10} + r_{11}\omega_{11}^2 \sin \theta_{11} - r_9\omega_9^2 \sin \theta_9 \end{vmatrix}$$

Loop 2

$$\begin{aligned} -r_7\alpha_7 \sin \theta_7 + r_3\alpha_3 \sin \theta_3 &= r_8\alpha_8 \sin \theta_8 + r_8\omega_8^2 \cos \theta_8 \\ &+ r_7\omega_7^2 \cos \theta_7 - r_3\omega_3^2 \cos \theta_3 \end{aligned} \quad (4.11a)$$

$$\begin{aligned} r_7\alpha_7 \cos \theta_7 - r_3\alpha_3 \cos \theta_3 &= -r_8\alpha_8 \cos \theta_8 + r_8\omega_8^2 \sin \theta_8 \\ &+ r_7\omega_7^2 \sin \theta_7 - r_3\omega_3^2 \sin \theta_3 \end{aligned} \quad (4.11b)$$

where α_7 and α_3 are unknown angular accelerations of links 5 and 7, respectively, and $\alpha_8 = \alpha_9$ is angular acceleration of link 4 which is obtained after the angular acceleration analysis of loop 1. Similarly, with Cramer's rule, we have:

$$\alpha_7 = \frac{\Lambda_{21}}{\Lambda_2} \quad (4.12a)$$

$$\alpha_3 = \frac{\Lambda_{22}}{\Lambda_2} \quad (4.12b)$$

where

$$\Lambda_2 = \Delta_2$$

$$\Lambda_{21} = \begin{vmatrix} r_8 \alpha_8 \sin \theta_8 + r_8 \omega_8^2 \cos \theta_8 + r_7 \omega_7^2 \cos \theta_7 - r_3 \omega_3^2 \cos \theta_3 & r_3 \sin \theta_3 \\ -r_8 \alpha_8 \cos \theta_8 + r_8 \omega_8^2 \sin \theta_8 + r_7 \omega_7^2 \sin \theta_7 - r_3 \omega_3^2 \sin \theta_3 & -r_3 \cos \theta_3 \end{vmatrix}$$

$$\Lambda_{22} = \begin{vmatrix} -r_7 \sin \theta_7 & r_8 \alpha_8 \sin \theta_8 + r_8 \omega_8^2 \cos \theta_8 + r_7 \omega_7^2 \cos \theta_7 - r_3 \omega_3^2 \cos \theta_3 \\ r_7 \cos \theta_7 & -r_8 \alpha_8 \cos \theta_8 + r_8 \omega_8^2 \sin \theta_8 + r_7 \omega_7^2 \sin \theta_7 - r_3 \omega_3^2 \sin \theta_3 \end{vmatrix}$$

Loop 3

$$\begin{aligned} & -r_{16} \alpha_{16} \sin \theta_{16} + r_5 \alpha_5 \sin \theta_5 \\ & = -r_4 \alpha_4 \sin \theta_4 - r_4 \omega_4^2 \cos \theta_4 + r_{15} \alpha_{15} \sin \theta_{15} \\ & \quad + r_{15} \omega_{15}^2 \cos \theta_{15} + r_{16} \omega_{16}^2 \cos \theta_{16} - r_5 \omega_5^2 \cos \theta_5 \end{aligned} \quad (4.13a)$$

$$\begin{aligned} & r_{16} \alpha_{16} \cos \theta_{16} - r_5 \alpha_5 \cos \theta_5 \\ & = r_4 \alpha_4 \cos \theta_4 - r_4 \omega_4^2 \sin \theta_4 - r_{15} \alpha_{15} \cos \theta_{15} \\ & \quad + r_{15} \omega_{15}^2 \sin \theta_{15} + r_{16} \omega_{16}^2 \sin \theta_{16} - r_5 \omega_5^2 \sin \theta_5 \end{aligned} \quad (4.13b)$$

where α_{16} and α_5 are unknown angular accelerations of links 6 and 8, respectively, and $\alpha_4 = \alpha_3$ and $\alpha_{15} = \alpha_7$ are the angular accelerations of links 7 and 5. Again, with Cramer's rule, we have:

$$\alpha_{16} = \frac{\Lambda_{31}}{\Lambda_3} \quad (4.14a)$$

$$\alpha_5 = \frac{\Lambda_{32}}{\Lambda_3} \quad (4.14b)$$

where

$$\Lambda_3 = \Delta_3$$

$$\Lambda_{31} = \begin{vmatrix} \left(\begin{array}{l} -r_4 \alpha_4 \sin \theta_4 - r_4 \omega_4^2 \cos \theta_4 + r_{15} \alpha_{15} \sin \theta_{15} \\ + r_{15} \omega_{15}^2 \cos \theta_{15} + r_{16} \omega_{16}^2 \cos \theta_{16} - r_5 \omega_5^2 \cos \theta_5 \end{array} \right) & r_5 \sin \theta_5 \\ \left(\begin{array}{l} r_4 \alpha_4 \cos \theta_4 - r_4 \omega_4^2 \sin \theta_4 - r_{15} \alpha_{15} \cos \theta_{15} \\ + r_{15} \omega_{15}^2 \sin \theta_{15} + r_{16} \omega_{16}^2 \sin \theta_{16} - r_5 \omega_5^2 \sin \theta_5 \end{array} \right) & -r_5 \cos \theta_5 \end{vmatrix}$$

$$\Lambda_{32} = \begin{vmatrix} -r_{16} \sin \theta_{16} & \begin{pmatrix} -r_4 \alpha_4 \sin \theta_4 - r_4 \omega_4^2 \cos \theta_4 + r_{15} \alpha_{15} \sin \theta_{15} \\ + r_{15} \omega_{15}^2 \cos \theta_{15} + r_{16} \omega_{16}^2 \cos \theta_{16} - r_5 \omega_5^2 \cos \theta_5 \end{pmatrix} \\ r_{16} \cos \theta_{16} & \begin{pmatrix} r_4 \alpha_4 \cos \theta_4 - r_4 \omega_4^2 \sin \theta_4 - r_{15} \alpha_{15} \cos \theta_{15} \\ + r_{15} \omega_{15}^2 \sin \theta_{15} + r_{16} \omega_{16}^2 \sin \theta_{16} - r_5 \omega_5^2 \sin \theta_5 \end{pmatrix} \end{vmatrix}$$

Loop 4

$$\begin{aligned} & -r_{17} \alpha_{17} \sin \theta_{17} + r_{18} \alpha_{18} \sin \theta_{18} \\ & = -r_8 \alpha_8 \sin \theta_8 - r_8 \omega_8^2 \cos \theta_8 + r_9 \alpha_9 \sin \theta_9 \\ & \quad + r_9 \omega_9^2 \cos \theta_9 - r_7 \alpha_7 \sin \theta_7 - r_7 \omega_7^2 \cos \theta_7 \\ & \quad - r_{15} \alpha_{15} \sin \theta_{15} - r_{15} \omega_{15}^2 \cos \theta_{15} - r_{16} \alpha_{16} \sin \theta_{16} \\ & \quad - r_{16} \omega_{16}^2 \cos \theta_{16} - r_6 \alpha_6 \sin \theta_6 - r_6 \omega_6^2 \cos \theta_6 \\ & \quad + r_{12} \alpha_{12} \sin \theta_{12} + r_{12} \omega_{12}^2 \cos \theta_{12} + r_{17} \omega_{17}^2 \cos \theta_{17} - r_{18} \omega_{18}^2 \cos \theta_{18} \end{aligned} \tag{4.15a}$$

$$\begin{aligned} & r_{17} \alpha_{17} \cos \theta_{17} - r_{18} \alpha_{18} \cos \theta_{18} \\ & = r_8 \alpha_8 \cos \theta_8 - r_8 \omega_8^2 \sin \theta_8 - r_9 \alpha_9 \cos \theta_9 \\ & \quad + r_9 \omega_9^2 \sin \theta_9 + r_7 \alpha_7 \cos \theta_7 - r_7 \omega_7^2 \sin \theta_7 \\ & \quad + r_{15} \alpha_{15} \cos \theta_{15} - r_{15} \omega_{15}^2 \sin \theta_{15} + r_{16} \alpha_{16} \cos \theta_{16} \\ & \quad - r_{16} \omega_{16}^2 \sin \theta_{16} + r_6 \alpha_6 \cos \theta_6 - r_6 \omega_6^2 \sin \theta_6 \\ & \quad - r_{12} \alpha_{12} \cos \theta_{12} + r_{12} \omega_{12}^2 \sin \theta_{12} + r_{17} \omega_{17}^2 \sin \theta_{17} - r_{18} \omega_{18}^2 \sin \theta_{18} \end{aligned} \tag{4.15b}$$

where α_{17} and α_{18} are unknown angular accelerations of links 3 and 9, respectively, and $\alpha_6 = \alpha_5$ and $\alpha_{12} = \alpha_{11}$ are the angular accelerations of links 8 and 2. Then, we have:

$$\alpha_{17} = \frac{\Lambda_{41}}{\Lambda_4} \tag{4.16a}$$

$$\alpha_{18} = \frac{\Lambda_{42}}{\Lambda_4} \tag{4.16b}$$

where

$$\Lambda_4 = \Delta_4$$

$$\Lambda_{41} = \left(\begin{array}{l}
\left. \begin{array}{l}
-r_8\alpha_8 \sin \theta_8 - r_8\omega_8^2 \cos \theta_8 + r_9\alpha_9 \sin \theta_9 \\
+r_9\omega_9^2 \cos \theta_9 - r_7\alpha_7 \sin \theta_7 - r_7\omega_7^2 \cos \theta_7 \\
-r_{15}\alpha_{15} \sin \theta_{15} - r_{15}\omega_{15}^2 \cos \theta_{15} - r_{16}\alpha_{16} \sin \theta_{16} \\
-r_{16}\omega_{16}^2 \cos \theta_{16} - r_6\alpha_6 \sin \theta_6 - r_6\omega_6^2 \cos \theta_6 \\
+r_{12}\alpha_{12} \sin \theta_{12} + r_{12}\omega_{12}^2 \cos \theta_{12} + r_{17}\omega_{17}^2 \cos \theta_{17} \\
-r_{18}\omega_{18}^2 \cos \theta_{18}
\end{array} \right\} r_{18} \sin \theta_{18} \\
\left. \begin{array}{l}
r_8\alpha_8 \cos \theta_8 - r_8\omega_8^2 \sin \theta_8 - r_9\alpha_9 \cos \theta_9 \\
+r_9\omega_9^2 \sin \theta_9 + r_7\alpha_7 \cos \theta_7 - r_7\omega_7^2 \sin \theta_7 \\
+r_{15}\alpha_{15} \cos \theta_{15} - r_{15}\omega_{15}^2 \sin \theta_{15} + r_{16}\alpha_{16} \cos \theta_{16} \\
-r_{16}\omega_{16}^2 \sin \theta_{16} + r_6\alpha_6 \cos \theta_6 - r_6\omega_6^2 \sin \theta_6 \\
-r_{12}\alpha_{12} \cos \theta_{12} + r_{12}\omega_{12}^2 \sin \theta_{12} + r_{17}\omega_{17}^2 \sin \theta_{17} \\
-r_{18}\omega_{18}^2 \sin \theta_{18}
\end{array} \right\} -r_{18} \cos \theta_{18}
\end{array} \right)$$

$$\Lambda_{42} = \left(\begin{array}{l}
-r_{17} \sin \theta_{17} \left(\begin{array}{l}
-r_8\alpha_8 \sin \theta_8 - r_8\omega_8^2 \cos \theta_8 + r_9\alpha_9 \sin \theta_9 \\
+r_9\omega_9^2 \cos \theta_9 - r_7\alpha_7 \sin \theta_7 - r_7\omega_7^2 \cos \theta_7 \\
-r_{15}\alpha_{15} \sin \theta_{15} - r_{15}\omega_{15}^2 \cos \theta_{15} - r_{16}\alpha_{16} \sin \theta_{16} \\
-r_{16}\omega_{16}^2 \cos \theta_{16} - r_6\alpha_6 \sin \theta_6 - r_6\omega_6^2 \cos \theta_6 \\
+r_{12}\alpha_{12} \sin \theta_{12} + r_{12}\omega_{12}^2 \cos \theta_{12} + r_{17}\omega_{17}^2 \cos \theta_{17} \\
-r_{18}\omega_{18}^2 \cos \theta_{18}
\end{array} \right) \\
r_{17} \cos \theta_{17} \left(\begin{array}{l}
r_8\alpha_8 \cos \theta_8 - r_8\omega_8^2 \sin \theta_8 - r_9\alpha_9 \cos \theta_9 \\
+r_9\omega_9^2 \sin \theta_9 + r_7\alpha_7 \cos \theta_7 - r_7\omega_7^2 \sin \theta_7 \\
+r_{15}\alpha_{15} \cos \theta_{15} - r_{15}\omega_{15}^2 \sin \theta_{15} + r_{16}\alpha_{16} \cos \theta_{16} \\
-r_{16}\omega_{16}^2 \sin \theta_{16} + r_6\alpha_6 \cos \theta_6 - r_6\omega_6^2 \sin \theta_6 \\
-r_{12}\alpha_{12} \cos \theta_{12} + r_{12}\omega_{12}^2 \sin \theta_{12} + r_{17}\omega_{17}^2 \sin \theta_{17} \\
-r_{18}\omega_{18}^2 \sin \theta_{18}
\end{array} \right)
\end{array} \right)$$

4.3 Velocities and Accelerations of the Mass Centers of Links

At first, we determine the relative position vector of the mass center of each moving link of the leg mechanism to locate the mass center position of each link related to a specific pivot on this link. These determinations of position vectors are based on that each link consists of homogeneous material such that the position of mass center of each link locates at the centroid of the link. These vectors are shown in Fig. 4.1 and listed

below.

$$\begin{aligned}\bar{L}_1 &= \frac{1}{2} \bar{r}_{10} \\ &= \frac{1}{2} r_{10} \cos \theta_{10} \hat{i} + \frac{1}{2} r_{10} \sin \theta_{10} \hat{j}\end{aligned}$$

$$\begin{aligned}\bar{L}_2 &= \frac{1}{3} \bar{r}_{11} + \frac{1}{3} (\bar{r}_{11} + \bar{r}_{12}) \\ &= \left(\frac{2}{3} r_{11} \cos \theta_{11} + \frac{1}{3} r_{12} \cos \theta_{12} \right) \hat{i} + \left(\frac{2}{3} r_{11} \sin \theta_{11} + \frac{1}{3} r_{12} \sin \theta_{12} \right) \hat{j}\end{aligned}$$

$$\begin{aligned}\bar{L}_3 &= \frac{1}{2} \bar{r}_{17} \\ &= \frac{1}{2} r_{17} \cos \theta_{17} \hat{i} + \frac{1}{2} r_{17} \sin \theta_{17} \hat{j}\end{aligned}$$

$$\begin{aligned}\bar{L}_4 &= \frac{1}{3} \bar{r}_9 + \frac{1}{3} \bar{r}_8 \\ &= \left(\frac{1}{3} r_9 \cos \theta_9 + \frac{1}{3} r_8 \cos \theta_8 \right) \hat{i} + \left(\frac{1}{3} r_9 \sin \theta_9 + \frac{1}{3} r_8 \sin \theta_8 \right) \hat{j}\end{aligned}$$

$$\begin{aligned}\bar{L}_5 &= \frac{1}{3} \bar{r}_7 + \frac{1}{3} (\bar{r}_7 + \bar{r}_{15}) \\ &= \left(\frac{2}{3} r_7 \cos \theta_7 + \frac{1}{3} r_{15} \cos \theta_{15} \right) \hat{i} + \left(\frac{2}{3} r_7 \sin \theta_7 + \frac{1}{3} r_{15} \sin \theta_{15} \right) \hat{j}\end{aligned}$$

$$\begin{aligned}\bar{L}_6 &= \frac{1}{2} \bar{r}_{16} \\ &= \frac{1}{2} r_{16} \cos \theta_{16} \hat{i} + \frac{1}{2} r_{16} \sin \theta_{16} \hat{j}\end{aligned}$$

$$\begin{aligned}\bar{L}_7 &= \frac{1}{3} \bar{r}_3 + \frac{1}{3} (\bar{r}_3 + \bar{r}_4) \\ &= \left(\frac{2}{3} r_3 \cos \theta_3 + \frac{1}{3} r_4 \cos \theta_4 \right) \hat{i} + \left(\frac{2}{3} r_3 \sin \theta_3 + \frac{1}{3} r_4 \sin \theta_4 \right) \hat{j}\end{aligned}$$

$$\begin{aligned}\bar{L}_8 &= \frac{1}{3} \bar{r}_5 + \frac{1}{3} (\bar{r}_5 + \bar{r}_6) \\ &= \left(\frac{2}{3} r_5 \cos \theta_5 + \frac{1}{3} r_6 \cos \theta_6 \right) \hat{i} + \left(\frac{2}{3} r_5 \sin \theta_5 + \frac{1}{3} r_6 \sin \theta_6 \right) \hat{j}\end{aligned}$$

$$\begin{aligned}\bar{L}_9 &= \frac{1}{2} \bar{r}_{18} \\ &= \frac{1}{2} r_{18} \cos \theta_{18} \hat{i} + \frac{1}{2} r_{18} \sin \theta_{18} \hat{j}\end{aligned}$$

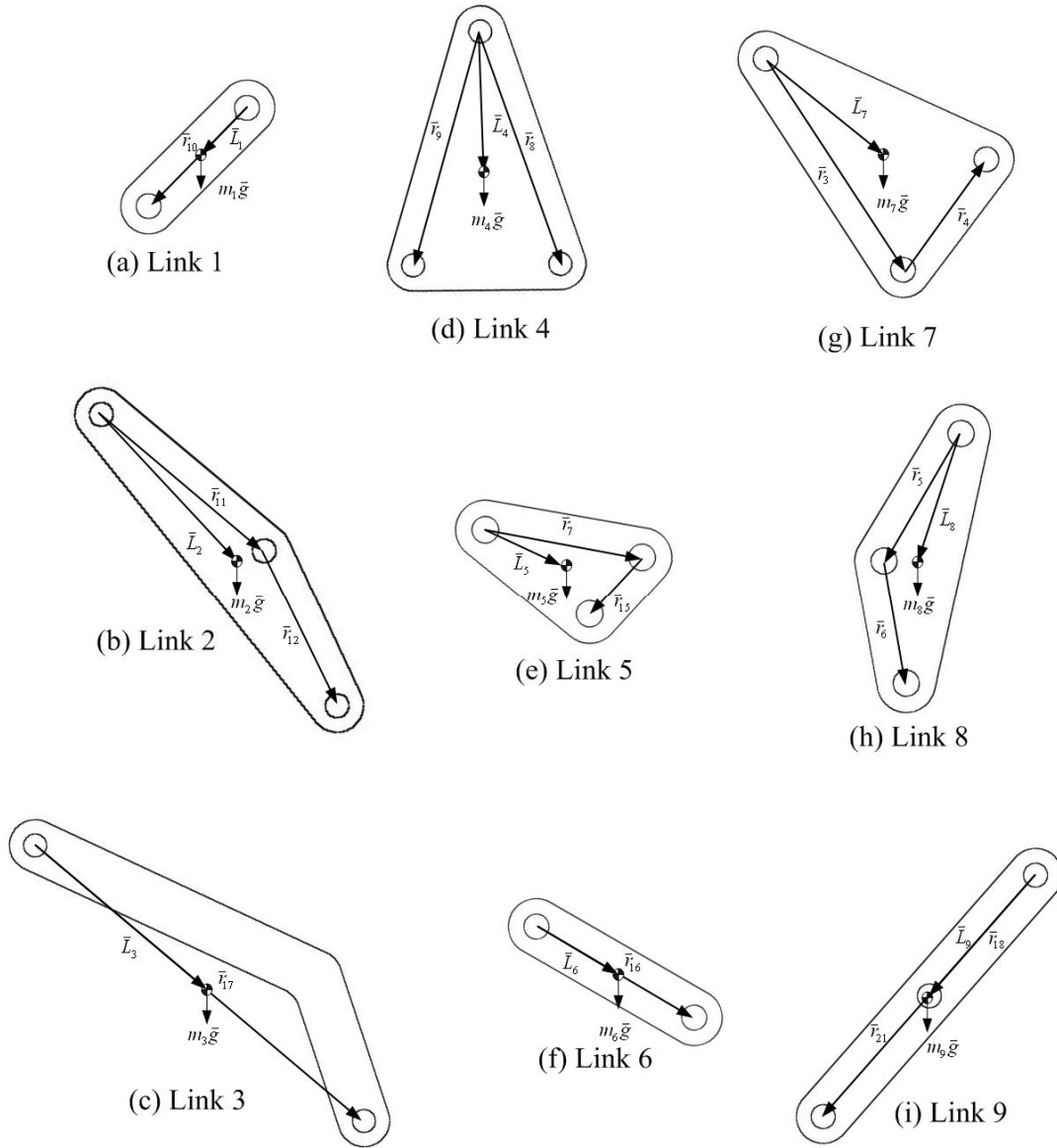


Figure 4.1 Position vectors of mass centers relative to the specific pivots

The center position of each link with respect to the body fixed coordinate system X_1Y_1 can be determined by the vectors as follows:

$$\bar{R}_{g_1} = \bar{L}_1 = \frac{1}{2} \bar{r}_{10}$$

$$\bar{R}_{g_2} = \bar{r}_{10} + \bar{L}_2 = \bar{r}_{10} + \frac{2}{3} \bar{r}_{11} + \frac{1}{3} \bar{r}_{12}$$

$$\bar{R}_{g_3} = \bar{r}_{10} + \bar{r}_{11} + \bar{r}_{12} + \bar{L}_3 = \bar{r}_{10} + \bar{r}_{11} + \bar{r}_{12} + \frac{1}{2} \bar{r}_{17}$$

$$\bar{R}_{g_4} = \bar{r}_1 + \bar{L}_4 = \bar{r}_1 + \frac{1}{3}\bar{r}_8 + \frac{1}{3}\bar{r}_9$$

$$\bar{R}_{g_5} = \bar{r}_1 + \bar{r}_8 + \bar{L}_5 = \bar{r}_1 + \bar{r}_8 + \frac{2}{3}\bar{r}_7 + \frac{1}{3}\bar{r}_{15}$$

$$\bar{R}_{g_6} = \bar{r}_1 + \bar{r}_8 + \bar{r}_7 + \bar{r}_{15} + \bar{L}_6 = \bar{r}_1 + \bar{r}_8 + \bar{r}_7 + \bar{r}_{15} + \frac{1}{2}\bar{r}_{16}$$

$$\bar{R}_{g_7} = \bar{r}_1 + \bar{r}_2 + \bar{L}_7 = \bar{r}_1 + \bar{r}_2 + \frac{2}{3}\bar{r}_3 + \frac{1}{3}\bar{r}_4$$

$$\bar{R}_{g_8} = \bar{r}_1 + \bar{r}_2 + \bar{r}_3 + \bar{r}_4 + \bar{L}_8 = \bar{r}_1 + \bar{r}_2 + \bar{r}_3 + \bar{r}_4 + \frac{2}{3}\bar{r}_5 + \frac{1}{3}\bar{r}_6$$

$$\bar{R}_{g_9} = \bar{r}_1 + \bar{r}_2 + \bar{r}_3 + \bar{r}_4 + \bar{r}_5 + \bar{r}_6 + \bar{L}_9 = \bar{r}_1 + \bar{r}_2 + \bar{r}_3 + \bar{r}_4 + \bar{r}_5 + \bar{r}_6 + \frac{1}{2}\bar{r}_{18}$$

And, the position of the foot point relative to the body fixed coordinate X_1Y_1 is:

$$\bar{R}_p = \bar{r}_1 + \bar{r}_2 + \bar{r}_3 + \bar{r}_4 + \bar{r}_5 + \bar{r}_6 + \bar{r}_{21}$$

The velocity and acceleration of the mass center of each link can be obtained by differentiating the above position vectors with respect to time once and twice, respectively.

And, so are the velocity and acceleration of the foot point.

4.4 Summary

In this chapter, the kinematic analysis of each link of the leg mechanism is performed, and the mathematical formulations are developed and presented. From the results of the kinematic analysis, the completed force analysis including the static force and dynamic force can be performed in next chapter.

Chapter 5

Force Analysis

In this chapter, the force equilibrium equations of links are derived to perform kinetostatic analysis [27, 28] for the joint forces, the output friction force, and the driving torque. Furthermore, based on the definition of mechanical advantage, the ratio of the input force and the output force, we could realize the transmissibility of force of the leg mechanism.

5.1 Force Analysis

Since the walking machine has the wave gait when it moves forward, it always retains at least three feet on the ground simultaneously all the time when it translates. Based on this fact, some assumptions are made to simplify the analysis:

1. The mass center of the walking machine is located at the central point of the body (the center of the ground link); that is, the weight of the walking machine concentrates on the rotating center of the driving gear.
2. The weight is distributed equally on the feet (three or four feet) touching the ground and results in reaction normal forces acting on these feet. The quantity of feet touching the ground at the specific time period could be decided by the phase of each foot, Fig.5.1.

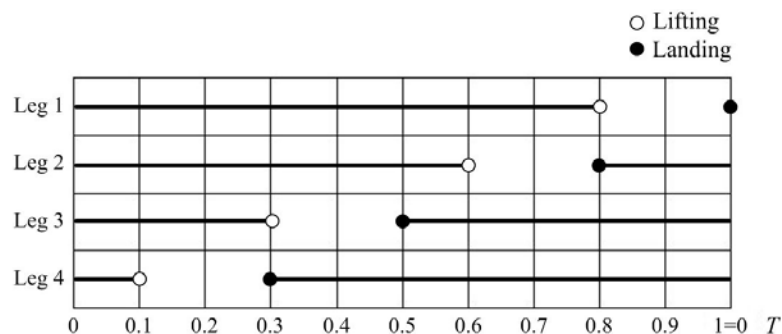


Figure 5.1 The gait diagram of the designed walking machine with the duty factor of 0.8

3. The mass center of each link of the walking machine is located at the centroid of the link.
4. The frictions of joints between the adjacent links are neglected.

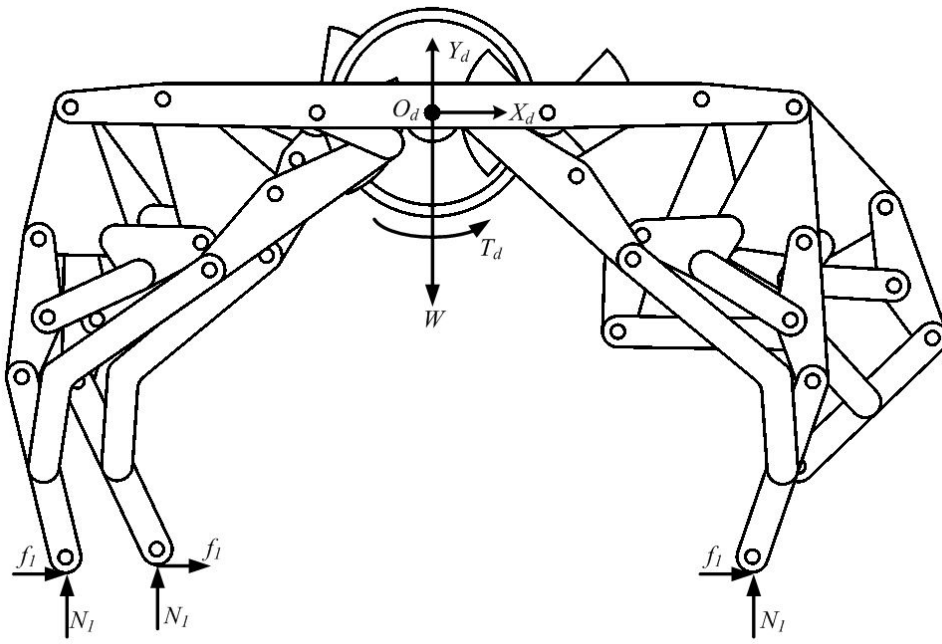
Figs. 5.2(a) and (b) show the external loads on the walking machine when there are three and four feet on the ground, respectively; where W is the total weight of the walking machine, T_d is the driving torque, f_1 is the friction between the foot and ground when there are three feet on the ground, f_2 is the friction between the foot and ground when there are four feet on the ground, N_1 is the normal force of the supporting leg when there are three feet on the ground, and N_2 is the normal force of the supporting leg when there are four feet on the ground.

Figs. 5.3(a) ~ (i) show the free body diagram of each moving link. Here, \vec{T}_n is the driving torque on the crank of leg n ($n=1 \sim 4$), \vec{F}_{ij} (for $i=0 \sim 9$, $j=0 \sim 9$, and $i \neq j$) is the joint force exerting on the joint incident with the links i and j . Vector \vec{r}_k ($k=3 \sim 22$) represents the size, including the shape and edge length, of each moving link. \vec{L}_i ($i=1 \sim 9$), as expressed in Chapter 4, indicates the relative position of mass center of each moving link. And, $m_i \vec{g}$ ($i=1 \sim 9$) is the weight of each moving link.

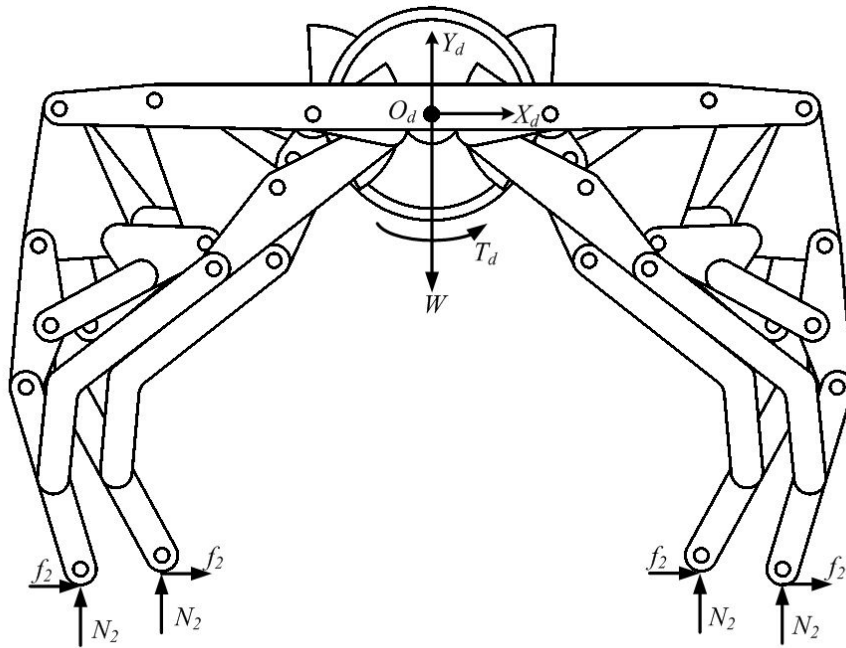
Figs. 5.4(a) ~ (i) show the kinetic diagram of each moving link; where $m_i(\vec{a}_{G_i})_x$ and $m_i(\vec{a}_{G_i})_y$ ($i=1 \sim 9$) are the components of the inertia force of each moving link, $I_{G_i} \ddot{\phi}_i$ ($i=1 \sim 9$) is the kinetic moment of each moving link, and $\ddot{\phi}_i$ ($i=1 \sim 9$) is the angular acceleration of each moving link.

5.1.1 Static Force Analysis

According to Figs. 5.2 and 5.3, and by assuming that each link has no mass and the walking machine is subjected to the external normal forces and frictions on the feet, the force equilibrium equations can be solved for the nine moving links as follows:



(a) Three feet on the ground



(b) Four feet on the ground

Figure 5.2 External loads on the walking machine

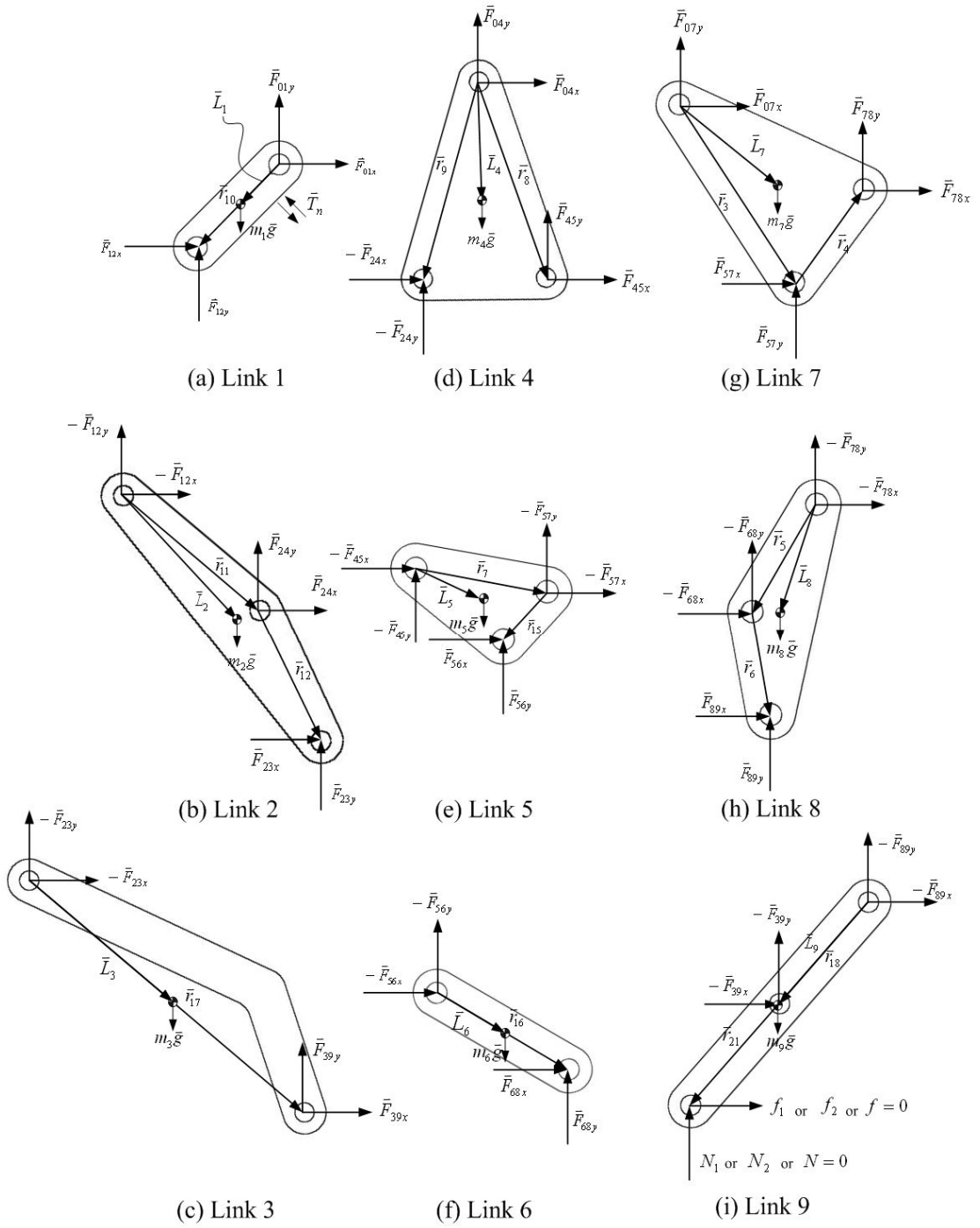


Figure 5.3 Free body diagram of each moving link

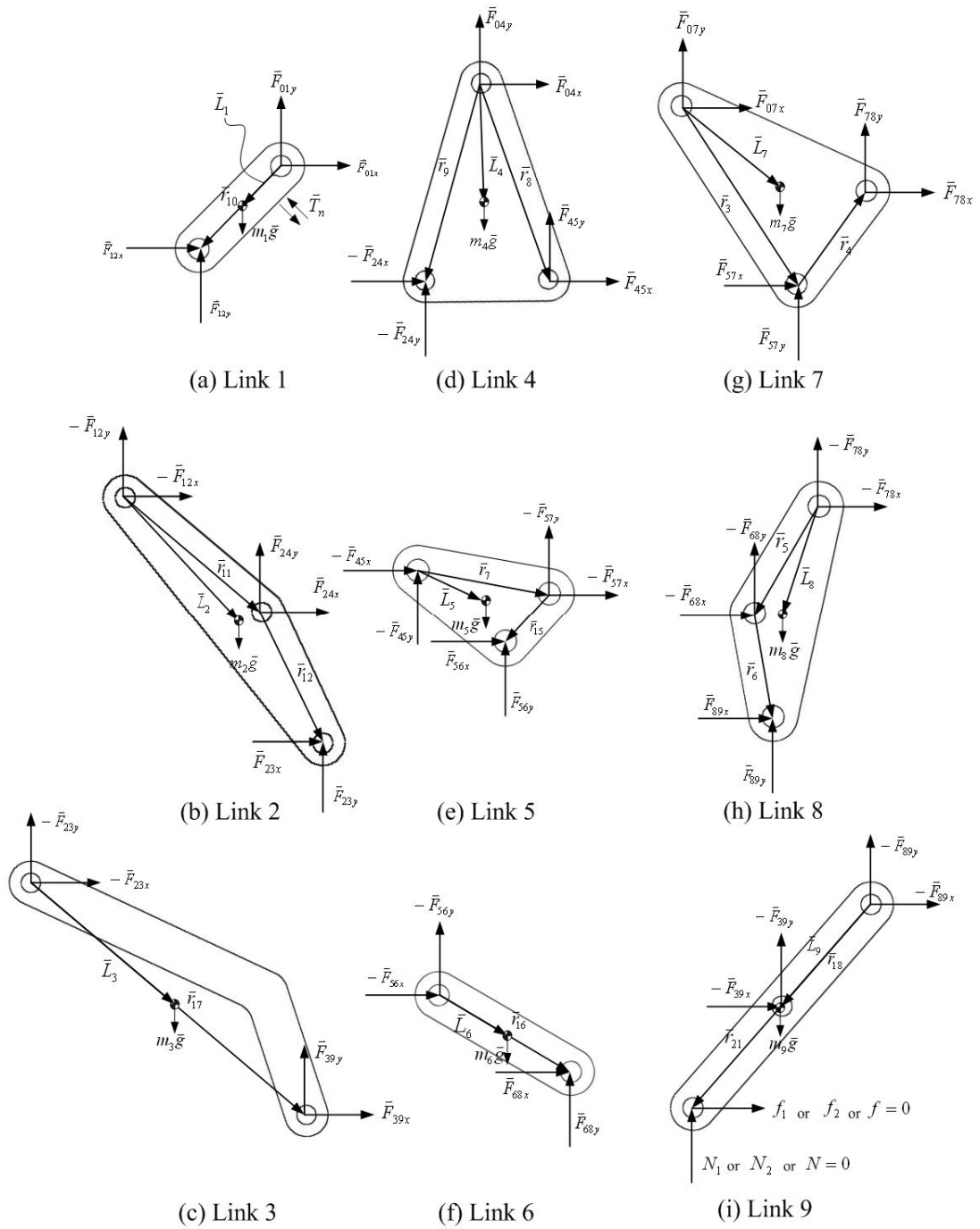


Figure 5.4 Kinetic diagram of each moving link

Link 1

$$\rightarrow \sum F_x = 0 \Rightarrow F_{01x} + F_{12x} = 0 \quad (5.1a)$$

$$+\uparrow \sum F_y = 0 \Rightarrow F_{01y} + F_{12y} = 0 \quad (5.1b)$$

$$+\curvearrowright \sum M = 0 \Rightarrow r_{10} \cos \theta_{10} F_{12y} - r_{10} \sin \theta_{10} F_{12x} + T_n = 0 \quad (5.1c)$$

Link 2

$$\rightarrow \sum F_x = 0 \Rightarrow -F_{12x} + F_{24x} + F_{23x} = 0 \quad (5.2a)$$

$$+\uparrow \sum F_y = 0 \Rightarrow -F_{12y} + F_{24y} + F_{23y} = 0 \quad (5.2b)$$

$$+\curvearrowright \sum M = 0 \Rightarrow r_{11} \cos \theta_{11} F_{24y} - r_{11} \sin \theta_{11} F_{24x} + (r_{11} \cos \theta_{11} + r_{12} \cos \theta_{12}) F_{23y} \quad (5.2c)$$

$$- (r_{11} \sin \theta_{11} + r_{12} \sin \theta_{12}) F_{23x} = 0$$

Link 3

$$\rightarrow \sum F_x = 0 \Rightarrow -F_{23x} + F_{39x} = 0 \quad (5.3a)$$

$$+\uparrow \sum F_y = 0 \Rightarrow -F_{23y} + F_{39y} = 0 \quad (5.3b)$$

$$+\curvearrowright \sum M = 0 \Rightarrow r_{17} \cos \theta_{17} F_{39y} - r_{17} \sin \theta_{17} F_{39x} = 0 \quad (5.3c)$$

Link 4

$$\rightarrow \sum F_x = 0 \Rightarrow F_{04x} - F_{24x} + F_{45x} = 0 \quad (5.4a)$$

$$+\uparrow \sum F_y = 0 \Rightarrow F_{04y} - F_{24y} + F_{45y} = 0 \quad (5.4b)$$

$$+\curvearrowright \sum M = 0 \Rightarrow r_9 \cos \theta_9 (-F_{24y}) - r_9 \sin \theta_9 (-F_{24x}) \quad (5.4c)$$

$$+ r_8 \cos \theta_8 F_{45y} - r_8 \sin \theta_8 F_{45x} = 0$$

Link 5

$$\begin{array}{l} + \\ \rightarrow \end{array} \sum F_x = 0 \Rightarrow -F_{45x} - F_{57x} + F_{56x} = 0 \quad (5.5a)$$

$$\begin{array}{l} + \\ \uparrow \end{array} \sum F_y = 0 \Rightarrow -F_{45y} - F_{57y} + F_{56y} = 0 \quad (5.5b)$$

$$\begin{array}{l} + \\ \curvearrowright \end{array} \sum M = 0 \Rightarrow r_7 \cos \theta_7 (-F_{57y}) - r_7 \sin \theta_7 (-F_{57x}) \quad (5.5c)$$

$$+ (r_7 \cos \theta_7 + r_{15} \cos \theta_{15}) F_{56y} - (r_7 \sin \theta_7 + r_{15} \sin \theta_{15}) F_{56x} = 0$$

Link 6

$$\begin{array}{l} + \\ \rightarrow \end{array} \sum F_x = 0 \Rightarrow -F_{56x} + F_{68x} = 0 \quad (5.6a)$$

$$\begin{array}{l} + \\ \uparrow \end{array} \sum F_y = 0 \Rightarrow -F_{56y} + F_{68y} = 0 \quad (5.6b)$$

$$\begin{array}{l} + \\ \curvearrowright \end{array} \sum M = 0 \Rightarrow r_{16} \cos \theta_{16} F_{68y} - r_{16} \sin \theta_{16} F_{68x} = 0 \quad (5.6c)$$

Link 7

$$\begin{array}{l} + \\ \rightarrow \end{array} \sum F_x = 0 \Rightarrow F_{07x} + F_{78x} + F_{57x} = 0 \quad (5.7a)$$

$$\begin{array}{l} + \\ \uparrow \end{array} \sum F_y = 0 \Rightarrow F_{07y} + F_{78y} + F_{57y} = 0 \quad (5.7b)$$

$$\begin{array}{l} + \\ \curvearrowright \end{array} \sum M = 0 \Rightarrow r_3 \cos \theta_3 F_{57y} - r_3 \sin \theta_3 F_{57x} + (r_3 \cos \theta_3 + r_4 \cos \theta_4) F_{78y} \quad (5.7c)$$

$$- (r_3 \sin \theta_3 + r_4 \sin \theta_4) F_{78x} = 0$$

Link 8

$$\begin{array}{l} + \\ \rightarrow \end{array} \sum F_x = 0 \Rightarrow -F_{78x} - F_{68x} + F_{89x} = 0 \quad (5.8a)$$

$$\begin{array}{l} + \\ \uparrow \end{array} \sum F_y = 0 \Rightarrow -F_{78y} - F_{68y} + F_{89y} = 0 \quad (5.8b)$$

$$\begin{array}{l} + \\ \curvearrowright \end{array} \sum M = 0 \Rightarrow r_5 \cos \theta_5 (-F_{68y}) - r_5 \sin \theta_5 (-F_{68x}) \quad (5.8c)$$

$$+ (r_5 \cos \theta_5 + r_6 \cos \theta_6) F_{89y} - (r_5 \sin \theta_5 + r_6 \sin \theta_6) F_{89x} = 0$$

Link 9

$$\begin{array}{l} \xrightarrow{+} \sum F_x = 0 \Rightarrow -F_{89x} - F_{39x} + f = 0 \end{array} \quad (5.9a)$$

$$\begin{array}{l} +\uparrow \sum F_y = 0 \Rightarrow -F_{89y} - F_{39y} + N = 0 \end{array} \quad (5.9b)$$

$$\begin{array}{l} +\curvearrowright \sum M = 0 \Rightarrow r_{18} \cos \theta_{18} (-F_{39y}) - r_{18} \sin \theta_{18} (-F_{39x}) \\ \quad \quad \quad + r_{21} \cos \theta_{21} N - r_{21} \sin \theta_{21} f = 0 \end{array} \quad (5.9c)$$

where $N = N_1 = \frac{1}{3}W$ when there are three feet on the ground, $N = N_2 = \frac{1}{4}W$ when there are four feet on the ground, or $N = 0$ when the foot is at the transfer phase, i.e., the foot is in the air. For simplicity, the friction f is set equal to $\mu_s N$ where $\mu_s = 0.25$ for the contact between rubber and wood. Obviously, from above equations, we have 27 equations and 27 unknowns, so we are able to use Gauss elimination to solve for each joint force and the input driving torque on the crank (link 1). And, the results of the static force analysis of the four leg are shown in Fig. 5.5 with the computation parameters.

5.1.2 Inertia Force Analysis

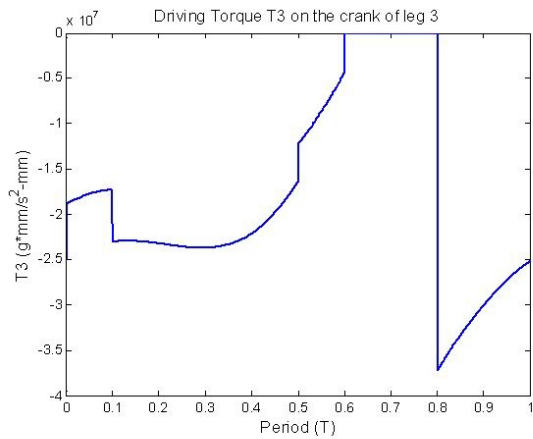
After the static force analysis, by assuming that there is no external load N and friction f on the feet, we perform the inertia force analysis. According to Figs. 5.1, 5.2, and 5.3, the force equilibrium equations for inertia force analysis can be solved for the nine moving links as follows:

Link 1

$$\begin{array}{l} \xrightarrow{+} \sum F_x = 0 \Rightarrow F_{01x} + F_{12x} = m_1 a_{G_1x} \end{array} \quad (5.10a)$$

$$\begin{array}{l} +\uparrow \sum F_y = 0 \Rightarrow F_{01y} + F_{12y} - m_1 g = m_1 a_{G_1y} \end{array} \quad (5.10b)$$

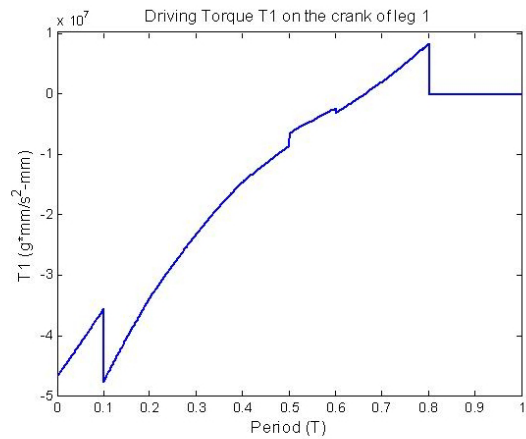
$$\begin{array}{l} +\curvearrowright \sum M = 0 \Rightarrow r_{10} \cos \theta_{10} F_{12y} - r_{10} \sin \theta_{10} F_{12x} + T_n + L_{1x} (-m_1 g) \\ \quad \quad \quad = m_1 (L_{1x} a_{G_1y} - L_{1y} a_{G_1x}) + I_{G_1} \ddot{\phi}_1 \end{array} \quad (5.10c)$$



Leg 3 :

$$\theta_{10}(T=0) = 22.75^{\circ}$$

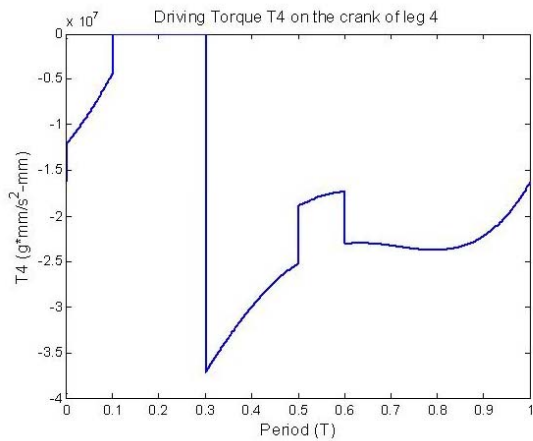
$$\omega_{10} = -11.625 \text{ deg/s (c.w.) @ } \theta_{10} = 46^{\circ} \sim 313^{\circ}$$

$$\omega_{10} = -139.5 \text{ deg/s (c.w.) @ } \theta_{10} = 312^{\circ} \sim 45^{\circ}$$


Leg 1 :

$$\theta_{10}(T=0) = 227^{\circ}$$

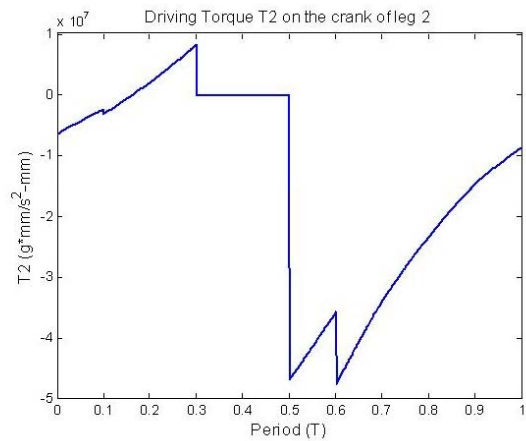
$$\omega_{10} = -11.625 \text{ deg/s (c.w.) @ } \theta_{10} = 227^{\circ} \sim 134^{\circ}$$

$$\omega_{10} = -139.5 \text{ deg/s (c.w.) @ } \theta_{10} = 135^{\circ} \sim 226^{\circ}$$


Leg 4 :

$$\theta_{10}(T=0) = 324.625^{\circ}$$

$$\omega_{10} = -11.625 \text{ deg/s (c.w.) @ } \theta_{10} = 46^{\circ} \sim 313^{\circ}$$

$$\omega_{10} = -139.5 \text{ deg/s (c.w.) @ } \theta_{10} = 312^{\circ} \sim 45^{\circ}$$


Leg 2 :

$$\theta_{10}(T=0) = 168.875^{\circ}$$

$$\omega_{10} = -11.625 \text{ deg/s (c.w.) @ } \theta_{10} = 227^{\circ} \sim 134^{\circ}$$

$$\omega_{10} = -139.5 \text{ deg/s (c.w.) @ } \theta_{10} = 135^{\circ} \sim 226^{\circ}$$

Figure 5.5 The results of static force analysis of the four legs

Link 2

$$\begin{aligned} \rightarrow \sum F_x = 0 \Rightarrow -F_{12x} + F_{24x} + F_{23x} = m_2 a_{G_2x} \end{aligned} \quad (5.11a)$$

$$\uparrow \sum F_y = 0 \Rightarrow -F_{12y} + F_{24y} + F_{23y} - m_2 g = m_2 a_{G_2y} \quad (5.11b)$$

$$\begin{aligned} \curvearrowright \sum M = 0 \Rightarrow r_{11} \cos \theta_{11} F_{24y} - r_{11} \sin \theta_{11} F_{24x} + (r_{11} \cos \theta_{11} + r_{12} \cos \theta_{12}) F_{23y} \\ - (r_{11} \sin \theta_{11} + r_{12} \sin \theta_{12}) F_{23x} - L_{2x} (-m_2 g) \\ = m_2 (L_{2x} a_{G_2y} - L_{2y} a_{G_2x}) + I_{G_2} \ddot{\phi}_2 \end{aligned} \quad (5.11c)$$

Link 3

$$\rightarrow \sum F_x = 0 \Rightarrow -F_{23x} + F_{39x} = m_3 a_{G_3x} \quad (5.12a)$$

$$\uparrow \sum F_y = 0 \Rightarrow -F_{23y} + F_{39y} - m_3 g = m_3 a_{G_3y} \quad (5.12b)$$

$$\begin{aligned} \curvearrowright \sum M = 0 \Rightarrow r_{17} \cos \theta_{17} F_{39y} - r_{17} \sin \theta_{17} F_{39x} - L_{3x} (-m_3 g) \\ = m_3 (L_{3x} a_{G_3y} - L_{3y} a_{G_3x}) + I_{G_3} \ddot{\phi}_3 \end{aligned} \quad (5.12c)$$

Link 4

$$\rightarrow \sum F_x = 0 \Rightarrow F_{04x} - F_{24x} + F_{45x} = m_4 a_{G_4x} \quad (5.13a)$$

$$\uparrow \sum F_y = 0 \Rightarrow F_{04y} - F_{24y} + F_{45y} - m_4 g = m_4 a_{G_4y} \quad (5.13b)$$

$$\begin{aligned} \curvearrowright \sum M = 0 \Rightarrow r_9 \cos \theta_9 (-F_{24y}) - r_9 \sin \theta_9 (-F_{24x}) \\ + r_8 \cos \theta_8 F_{45y} - r_8 \sin \theta_8 F_{45x} - L_{4x} (-m_4 g) \\ = m_4 (L_{4x} a_{G_4y} - L_{4y} a_{G_4x}) + I_{G_4} \ddot{\phi}_4 \end{aligned} \quad (5.13c)$$

Link 5

$$\rightarrow \sum F_x = 0 \Rightarrow -F_{45x} - F_{57x} + F_{56x} = m_5 a_{G_5x} \quad (5.14a)$$

$$\uparrow \sum F_y = 0 \Rightarrow -F_{45y} - F_{57y} + F_{56y} - m_5 g = m_5 a_{G_5y} \quad (5.14b)$$

$$\begin{aligned} \curvearrowright \sum M = 0 \Rightarrow r_7 \cos \theta_7 (-F_{57y}) - r_7 \sin \theta_7 (-F_{57x}) \\ + (r_7 \cos \theta_7 + r_{15} \cos \theta_{15}) F_{56y} - (r_7 \sin \theta_7 + r_{15} \sin \theta_{15}) F_{56x} \\ - L_{5x} (-m_5 g) = m_5 (L_{5x} a_{G_5y} - L_{5y} a_{G_5x}) + I_{G_5} \ddot{\phi}_5 \end{aligned} \quad (5.14c)$$

Link 6

$$\begin{array}{l} \rightarrow \\ + \end{array} \sum F_x = 0 \Rightarrow -F_{56x} + F_{68x} = m_6 a_{G_6x} \quad (5.15a)$$

$$\begin{array}{l} \uparrow \\ + \end{array} \sum F_y = 0 \Rightarrow -F_{56y} + F_{68y} - m_6 g = m_6 a_{G_6y} \quad (5.15b)$$

$$\begin{array}{l} \curvearrowright \\ + \end{array} \sum M = 0 \Rightarrow r_{16} \cos \theta_{16} F_{68y} - r_{16} \sin \theta_{16} F_{68x} - L_{6x}(-m_6 g) \\ = m_6 (L_{6x} a_{G_6y} - L_{6y} a_{G_6x}) + I_{G_6} \ddot{\phi}_6 \quad (5.15c)$$

Link 7

$$\begin{array}{l} \rightarrow \\ + \end{array} \sum F_x = 0 \Rightarrow F_{07x} + F_{78x} + F_{57x} = m_7 a_{G_7x} \quad (5.16a)$$

$$\begin{array}{l} \uparrow \\ + \end{array} \sum F_y = 0 \Rightarrow F_{07y} + F_{78y} + F_{57y} - m_7 g = m_7 a_{G_7y} \quad (5.16b)$$

$$\begin{array}{l} \curvearrowright \\ + \end{array} \sum M = 0 \Rightarrow r_3 \cos \theta_3 F_{57y} - r_3 \sin \theta_3 F_{57x} + (r_3 \cos \theta_3 + r_4 \cos \theta_4) F_{78y} \\ - (r_3 \sin \theta_3 + r_4 \sin \theta_4) F_{78x} - L_{7x}(-m_7 g) \\ = m_7 (L_{7x} a_{G_7y} - L_{7y} a_{G_7x}) + I_{G_7} \ddot{\phi}_7 \quad (5.16c)$$

Link 8

$$\begin{array}{l} \rightarrow \\ + \end{array} \sum F_x = 0 \Rightarrow -F_{78x} - F_{68x} + F_{89x} = m_8 a_{G_8x} \quad (5.17a)$$

$$\begin{array}{l} \uparrow \\ + \end{array} \sum F_y = 0 \Rightarrow -F_{78y} - F_{68y} + F_{89y} - m_8 g = m_8 a_{G_8y} \quad (5.17b)$$

$$\begin{array}{l} \curvearrowright \\ + \end{array} \sum M = 0 \Rightarrow r_5 \cos \theta_5 (-F_{68y}) - r_5 \sin \theta_5 (-F_{68x}) \\ + (r_5 \cos \theta_5 + r_6 \cos \theta_6) F_{89y} - (r_5 \sin \theta_5 + r_6 \sin \theta_6) F_{89x} \\ - L_{8x}(-m_8 g) = m_8 (L_{8x} a_{G_8y} - L_{8y} a_{G_8x}) + I_{G_8} \ddot{\phi}_8 \quad (5.17c)$$

Link 9

$$\begin{array}{l} \rightarrow \\ + \end{array} \sum F_x = 0 \Rightarrow -F_{89x} - F_{39x} = m_9 a_{G_9x} \quad (5.18a)$$

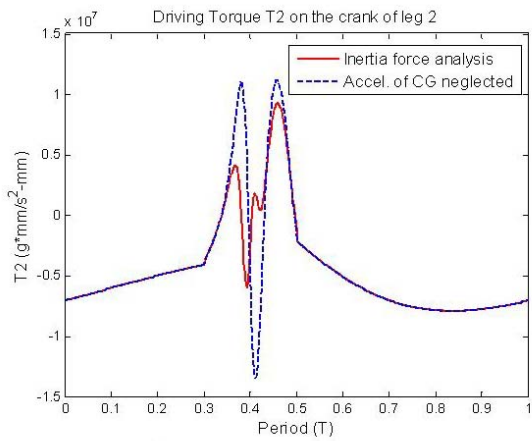
$$\begin{array}{l} \uparrow \\ + \end{array} \sum F_y = 0 \Rightarrow -F_{89y} - F_{39y} - m_9 g = m_9 a_{G_9y} \quad (5.18b)$$

$$\begin{array}{l} \curvearrowright \\ + \end{array} \sum M = 0 \Rightarrow r_{18} \cos \theta_{18} (-F_{39y}) - r_{18} \sin \theta_{18} (-F_{39x}) \\ + r_{21} \cos \theta_{21} N - r_{21} \sin \theta_{21} f - L_{9x}(-m_9 g) \\ = m_9 (L_{9x} a_{G_9y} - L_{9y} a_{G_9x}) + I_{G_9} \ddot{\phi}_9 \quad (5.18c)$$

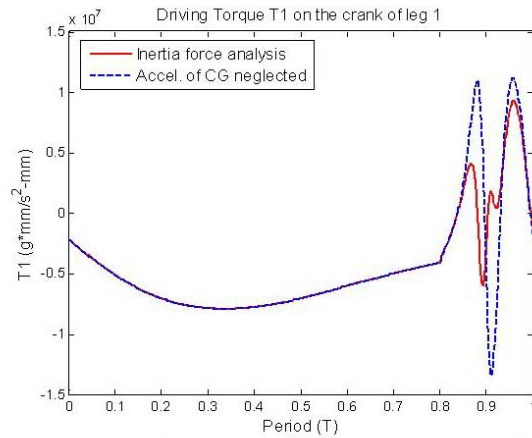
From Eqs. (5.10) ~ (5.18), there are 27 equations and 27 unknowns including the joint forces and the input driving torque on the crank. The number of equations matches that of unknowns, so we could use Gauss elimination to get the solutions. And, the results of inertia force analysis of the four legs are shown in Fig. 5.6 by the solid lines and compared with the results which the effect of accelerations of the mass centers is neglected. Even though the walking machine walks slowly, the effect of accelerations of the mass centers could not be neglected because of the angular velocity of the crank during the high-speed segment is twelve times of that during the low-speed segment.

5.1.3 Complete Result of Force Analysis

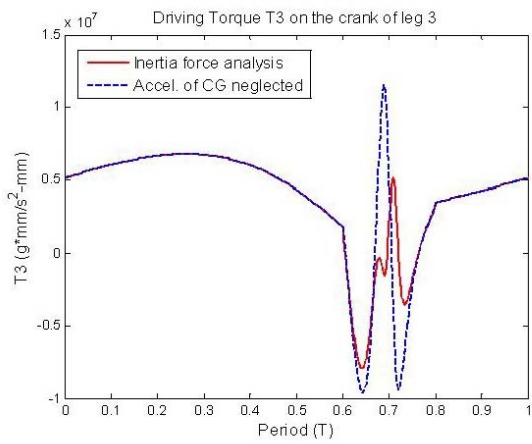
The complete result of force analysis of the four legs could be obtained by superposition of the result of static force analysis and that of inertia force analysis as shown in Fig 5.7. Because the concept of two-speed control is realized by using the gear train with fan-shaped gears, and the shafts of the double-layer fan-shaped gears are attached to the rotating shafts of the cranks of the four legs and the shaft of driving double-layer gear is attached to the shaft of the motor, the actual driving torque of the motor can be computed by knowing the speed ratio of the gear train. When the leg is at the support phase, the speed ratio between the driving gear and the fan-shaped gear is 3 to 1. On the other hand, when the leg is at the transfer phase, the speed ratio between the driving gear and the fan-shaped gear is 1 to 4. These two speed ratios make the rotating speed of the crank of the leg mechanism during the transfer phase as 12 times (about 11.48 times needed in Chapter 3) as that during the support phase. By knowing the two speed ratios of the gear train, the driving torques on the cranks of the four leg mechanisms are transferred to the shaft of the motor by these speed ratio as shown in Fig. 5.8a and the actual driving torque of the motor is obtained as shown in Fig. 5.8b.



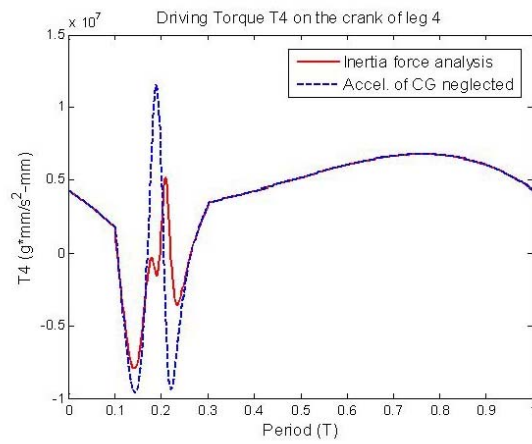
Leg 3 :
 $\theta_{10}(T=0) = 22.75^\circ$
 $\omega_{10} = -11.625 \text{ deg/s (c.w.) @ } \theta_{10} = 46^\circ \sim 313^\circ$
 $\omega_{10} = -139.5 \text{ deg/s (c.w.) @ } \theta_{10} = 312^\circ \sim 45^\circ$



Leg 1 :
 $\theta_{10}(T=0) = 227^\circ$
 $\omega_{10} = -11.625 \text{ deg/s (c.w.) @ } \theta_{10} = 227^\circ \sim 134^\circ$
 $\omega_{10} = -139.5 \text{ deg/s (c.w.) @ } \theta_{10} = 135^\circ \sim 226^\circ$

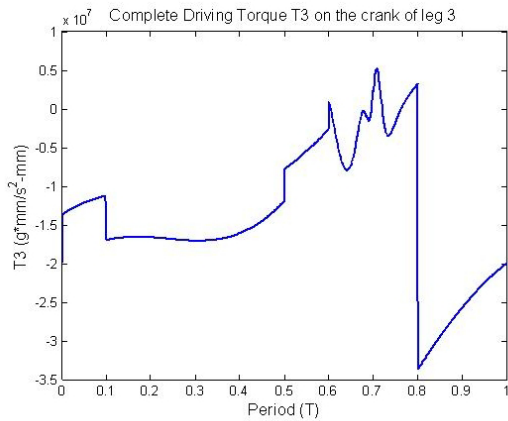


Leg 4 :
 $\theta_{10}(T=0) = 324.625^\circ$
 $\omega_{10} = -11.625 \text{ deg/s (c.w.) @ } \theta_{10} = 46^\circ \sim 313^\circ$
 $\omega_{10} = -139.5 \text{ deg/s (c.w.) @ } \theta_{10} = 312^\circ \sim 45^\circ$

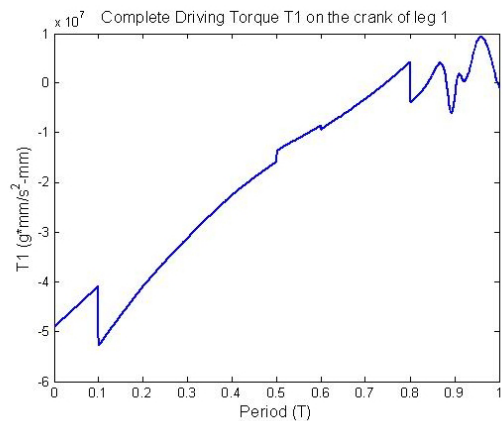


Leg 2 :
 $\theta_{10}(T=0) = 168.875^\circ$
 $\omega_{10} = -11.625 \text{ deg/s (c.w.) @ } \theta_{10} = 227^\circ \sim 134^\circ$
 $\omega_{10} = -139.5 \text{ deg/s (c.w.) @ } \theta_{10} = 135^\circ \sim 226^\circ$

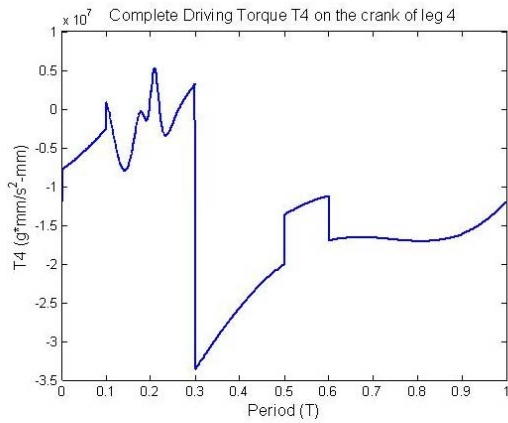
Figure 5.6 The results of inertia force analysis of the four legs



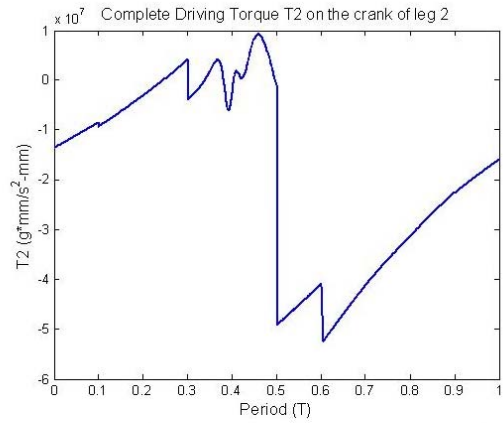
Leg 3 :
 $\theta_{10}(T=0) = 22.75^\circ$
 $\omega_{10} = -11.625 \text{ deg/s (c.w.) @ } \theta_{10} = 46^\circ \sim 313^\circ$
 $\omega_{10} = -139.5 \text{ deg/s (c.w.) @ } \theta_{10} = 312^\circ \sim 45^\circ$



Leg 1 :
 $\theta_{10}(T=0) = 227^\circ$
 $\omega_{10} = -11.625 \text{ deg/s (c.w.) @ } \theta_{10} = 227^\circ \sim 134^\circ$
 $\omega_{10} = -139.5 \text{ deg/s (c.w.) @ } \theta_{10} = 135^\circ \sim 226^\circ$

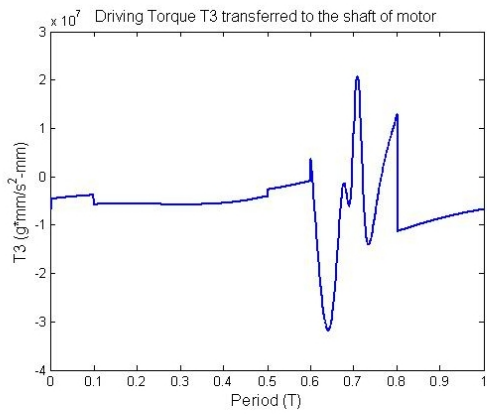


Leg 4 :
 $\theta_{10}(T=0) = 324.625^\circ$
 $\omega_{10} = -11.625 \text{ deg/s (c.w.) @ } \theta_{10} = 46^\circ \sim 313^\circ$
 $\omega_{10} = -139.5 \text{ deg/s (c.w.) @ } \theta_{10} = 312^\circ \sim 45^\circ$

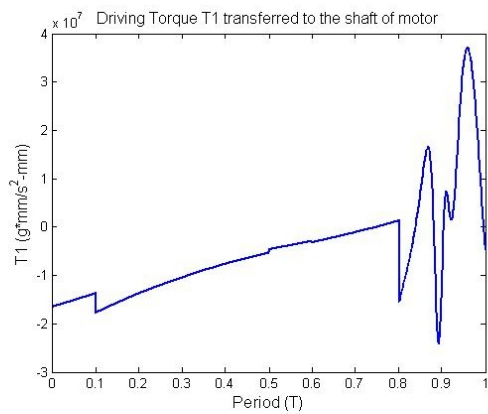


Leg 2 :
 $\theta_{10}(T=0) = 168.875^\circ$
 $\omega_{10} = -11.625 \text{ deg/s (c.w.) @ } \theta_{10} = 227^\circ \sim 134^\circ$
 $\omega_{10} = -139.5 \text{ deg/s (c.w.) @ } \theta_{10} = 135^\circ \sim 226^\circ$

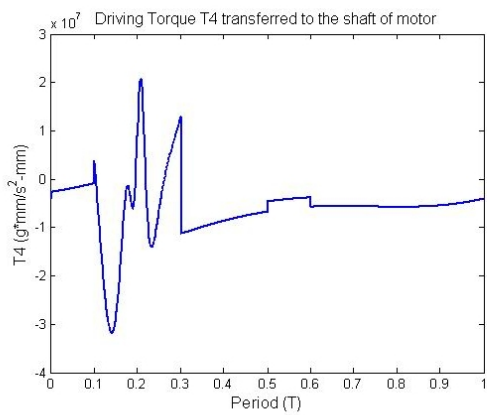
Figure 5.7 The complete results of force analysis of the four legs



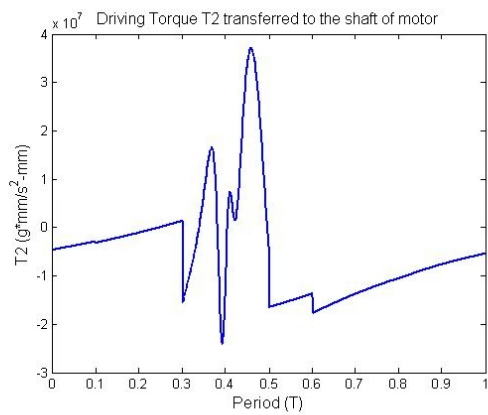
Leg 3



Leg 1

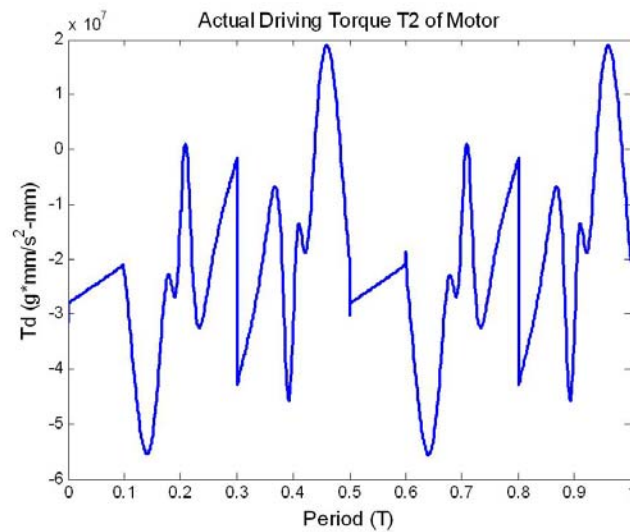


Leg 4



Leg 2

(a) The driving torques transferred to the shaft of the motor



(b) The actual driving torque of the motor

Figure 5.8 Driving torque on motor shaft

5.2 Mechanical Advantage

Machinery and mechanical devices, most of the time, should have good force, torque, or power transmissibility. In other words, frequently, a good machine or mechanical device should have high transmissibility of force or power. There must be some criteria to help designers to know the transmissibility of force or power such as mechanical advantage.

Mechanical advantage is such an important criterion that a designer must know to realize the transmissibility of force or torque of a particular machine or mechanism. The general definition of mechanical advantage, MA, is the ratio of the magnitude of the output force F_{out} and that of input force F_{in} [29]:

$$MA = \frac{F_{out}}{F_{in}} \quad (5.1)$$

For the linkage mechanism, the input force often applies on the input link which is adjacent to the ground link and the output force often carries out by the output link which is also adjacent to the ground link. When mechanical advantage is greater than one, it means that the particular mechanism works easily and has good transmissibility of force. On the other hand, when mechanical advantage is less than one, or even approaches to zero, the mechanism does not work smoothly or even can not work.

With regards to the walking machine which walks forward by pushing with hands, the input link is the cannon link (link 9) and the output link is the crank (link 1). However, as far as the walking machine which is driven by a motor as the power source is concerned, the input link is the crank (link 1) or the gear on the same axle of crank, and the output link is the cannon link (link 9) which has to produce sufficient normal force and friction to stop any slip and strides forwards. Therefore, for this walking machine driven by a motor as shown in Fig. 5.9, the driving force on the fan-shaped gear is the input force and the force vertical to link 9 is the output force.

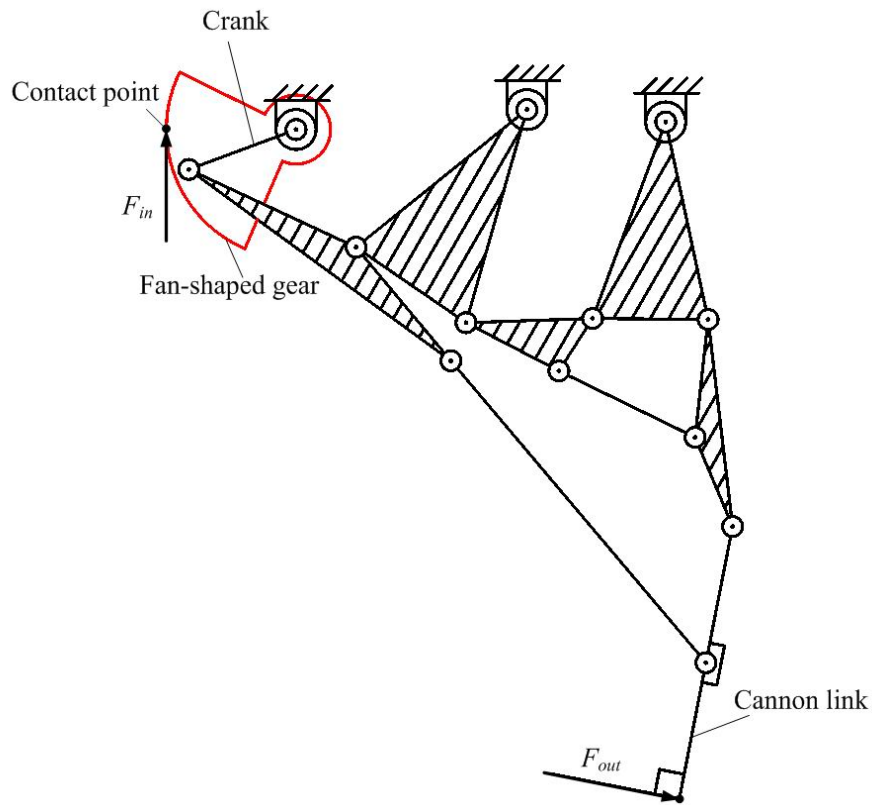


Figure 5.9 Input/output relation for the definition of mechanical advantage

5.3 Summary

In this chapter, the complete force analysis of the walking machine is performed. Even though the walking machine walks slowly, we do not ignore the effect of accelerations of the mass centers because of the ratio of speed during the high-speed segment and that during the low-speed segment. By the observation of mechanical advantage and the input force, we could tell whether the walking machine walks smoothly or not.

Chapter 6

Performance Analysis

Legged vehicle has the advantages to walk on the uneven terrain and to cross obstacles. However, one of the defects of the legged vehicle is that it is difficult to control the tossing during walking forwards because of its excellent stride. In this chapter, the ability of the walking machine to walking on level terrain, that to cross obstacles, and force transmissibility are investigated by analyzing the performance of the foot trajectory and mechanical advantage. At the same time, several comparisons with the Chiang's ten-bar linkage walking horse are made.

6.1 Evaluation of Foot Trajectory

The foot trajectory of Chiang's walking horse and that of this designed walking machine with ten-bar leg mechanisms on the basis of maximum leg extension of 200 mm at vertical direction are shown in Fig. 6.1. The distances of leg strokes and the heights of stride of these two walking machines are listed in Table 7.1 for comparison.

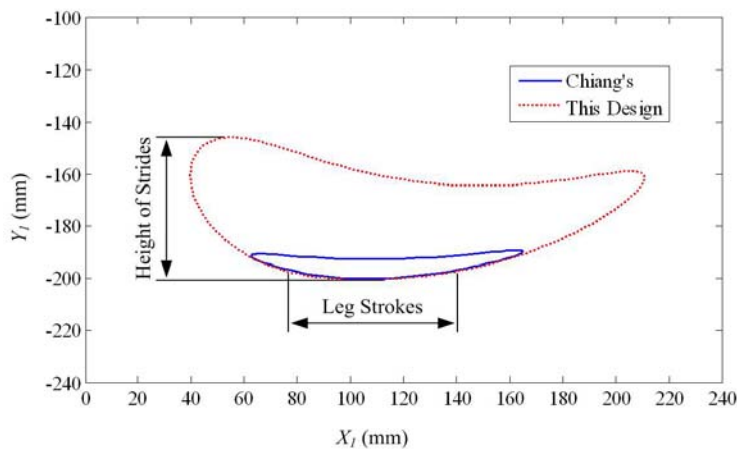


Figure 6.1 Comparison of foot trajectories

From Table 6.1, it is recognized that the leg stroke of the new designed walking machine with ten-bar leg mechanism is nearly the same as that of Chiang's and the height of stride of the new designed is much higher than that of Chiang's. That is, the new designed walking machine has better ability of striding.

Table 6.1 Comparison of foot trajectories

Machine Type	Leg Stroke	Height of Stride
This Design	63.03 mm	47.22 mm
Chiang's	62.10 mm	11.27 mm

6.2 Evaluation of Mechanical Advantage

Figure 6.2 shows the mechanical advantage of this designed walking machine. The mechanical advantage of this designed walking machine will not be compared with that of Chiang's. The reason is that, in name only, the input-output relations of the two walking machines are inverse; but in practice, the overall procedures of analyses are quite different. Therefore, in this section, the phenomena shown by the mechanical advantage in Fig. 6.2 is discussed.

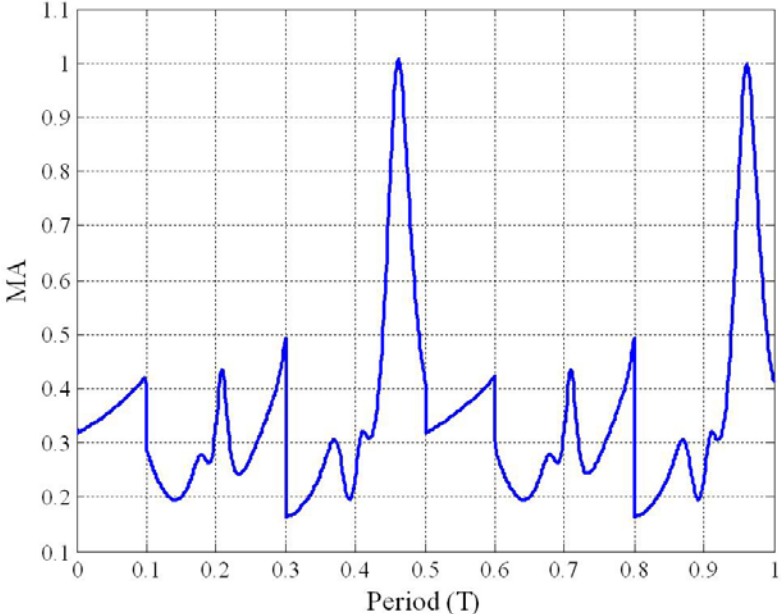


Figure 6.2 Mechanical advantage of the proposed walking machine

Fig. 6.2 reveals several discontinuities of sudden drop. These discontinuities are mainly caused by the changing of transferring legs. At these moments when the discontinuities appear, the walking machine is subjected to the discontinuous input-force from the fan-shaped gear. Except the discontinuities, the mechanical advantage appears in the form of curve oscillating up and down. At parts of time period, the loading of the driving motor is heavy because of low mechanical advantage. At most of the time period, the mechanical advantage oscillates and the walking machine is subjected to vibrations and undulations all the time. If the walking machine walks faster, the behaviors of vibration and undulation will be obvious.

6.3 Summary

This new designed walking machine with leg mechanism of 10-bar linkage is compared with Chiang's 10-link type wooden horse carriage between their foot trajectories. The new designed walking machine has obviously better ability of obstacle-crossing. Besides, the mechanical advantage of the new designed walking machine is executed that it is able to walk smoothly with small vibration and oscillation.

Chapter 7

Prototyping

In this chapter, a prototype of the designed walking machine with 10-bar linkage leg mechanism is built to verify the feasibility of its function and all the results of analyses in the previous chapters. At first, we arrange the layers of the links. Secondly, the detail sizes and shapes of links are designed and inputted into computer for simulation and animation. Then, the acrylic-plastic members of the leg mechanism are fabricated by an NC machining center. Finally, all parts of links are assembled to build up the leg mechanisms and we configure the driving gear train and a motor to complete the whole walking machine.

7.1 Layer Arrangement for Links

Since the layer arrangement affects so much on the strength of the leg mechanism, efficiency for power transmission, and interferences between links, it is a design procedure of great importance. Furthermore, friction between links and type of force transmission must be concerned for excellent layer arrangement. In order to obtain a robust layer arrangement, several points for attention are listed as follows:

1. The adjacent links can not be arranged on the same layer to avoid interference.
2. The friction at the interface between parts on adjacent layers must be reduced by cutting down the direct surface contact between the two parts.
3. The two parts which move across each other during the motion of mechanism should not be arranged on the same layer.
4. In order to increase space, reduce the complexity, make a compact design, and use fewer materials, fewer layers are preferred.

The front and rear leg mechanisms of the new type walking machine is unlike those of Chiang's walking horse with a carriage that the front and rear leg mechanisms of Chiang's

have the same crank. And, the front and rear leg mechanisms of this designed walking machine are much apart from each other. According the above two reasons, the interference between the front and rear leg mechanisms is not taken into consideration. With the application of method of arrangement for minimum number of layers [30], the layer arrangement is carried out according to the adjacency relation of links shown in Fig. 7.1. The corresponding linkage adjacent matrix for the leg mechanism is as follows [8]:

$$M_{LA} = \begin{bmatrix} 0 & R & I & I & R & I & I & R & I & I \\ R & 0 & R & 0 & 0 & 0 & 0 & 0 & 0 & 0 \\ I & R & 0 & R & R & 0 & 0 & 0 & 0 & 0 \\ I & 0 & R & 0 & 0 & 0 & 0 & 0 & 0 & R \\ R & 0 & R & 0 & 0 & R & 0 & 0 & 0 & 0 \\ I & 0 & 0 & 0 & R & 0 & R & R & 0 & 0 \\ I & 0 & 0 & 0 & 0 & R & 0 & I & R & 0 \\ R & 0 & 0 & 0 & 0 & R & I & 0 & R & 0 \\ I & 0 & 0 & 0 & 0 & 0 & R & R & 0 & R \\ I & 0 & 0 & R & 0 & 0 & 0 & 0 & R & 0 \end{bmatrix}$$

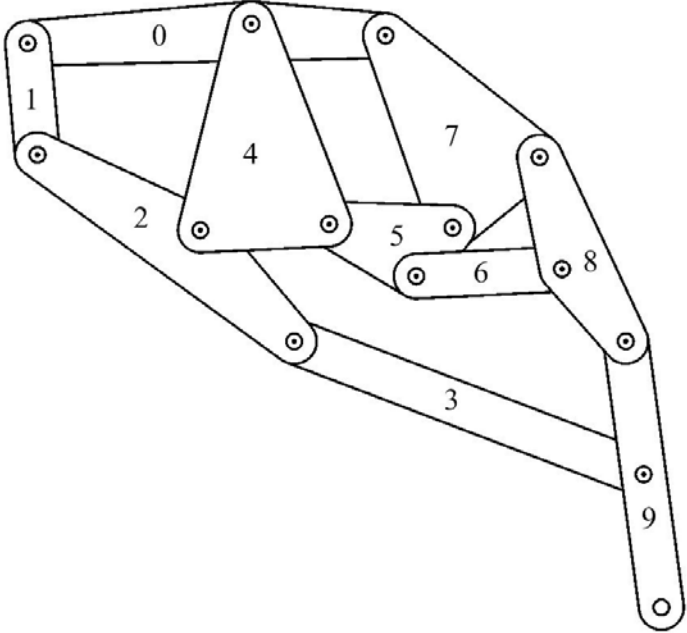


Figure 7.1 Skeleton of the leg mechanism

where R represents the two links hinged by a revolute joint and I means the two links interfere with each other. The frame is arranged on an independent layer; that is, it is supposed that all other links interfere with the frame. After this arrangement, the minimum number of layer arrangement for the leg mechanism of the new 10-link type walking machine is seven. To enhance the strength and robustness of leg mechanism, each link on the same leg mechanism is arranged double-deckedly. The final arrangement of links is shown in Table 7.1. And, the final arrangement is able to be recognized clearly from Fig. 7.2.

Table 7.1 Link arrangements for the prototype leg mechanism

Link \ Layer	I	II	III	IV	V	VI	VII	VIII	IX	X	XI	XII	XIII
0	⊙												⊙
1			⊙								⊙		
2				⊙						⊙			
3		⊙										⊙	
4							⊙						
5						⊙		⊙					
6					⊙				⊙				
7							⊙						
8						⊙		⊙					
9					⊙				⊙				

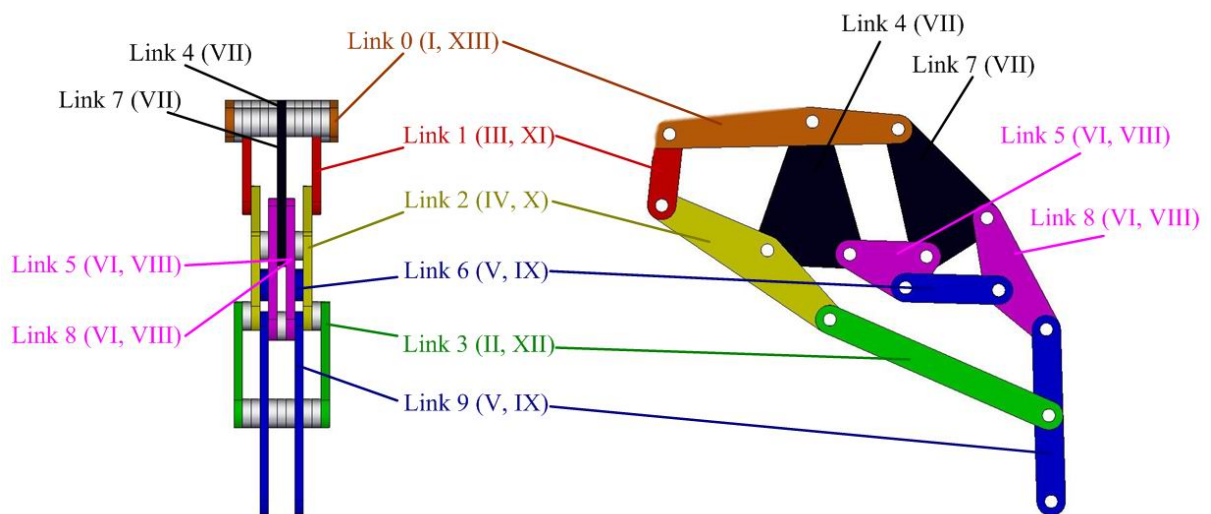


Figure 7.2 Final layer arrangement for links

7.2 Detail Design of Links and Fan-shaped Gears

According to the optimal size of each link, the exterior shape of each link is designed as shown in Fig. 7.3. The arc radius R_1 of frame, link 0, is 18.21 mm, and the arc radii R_2 of other links are 6.7 mm. The radius R_3 of the axle of revolute joint is 3 mm. Because of the requirement of the 11.48 times of speed ration between the high-speed segment during transfer phase and the low-speed segment during support phase, the double-layer spur gear and fan-shaped gear are designed as shown in Fig. 7.4. The gears have modulus of 1 mm and pressure angle of 20° , and mesh with the center distance of 50 mm. In Fig. 7.4, the solid circles represent the addendum circles and the dotted circles represent the pitch circles. And, the sizes and numbers of teeth of the gears are perceived. Note that the fan-shaped gear is cut off from the full-circle spur gears with gear of 75 teeth and pinion of 20 teeth. Fig. 7.5 shows the assembly of the new walking machine.

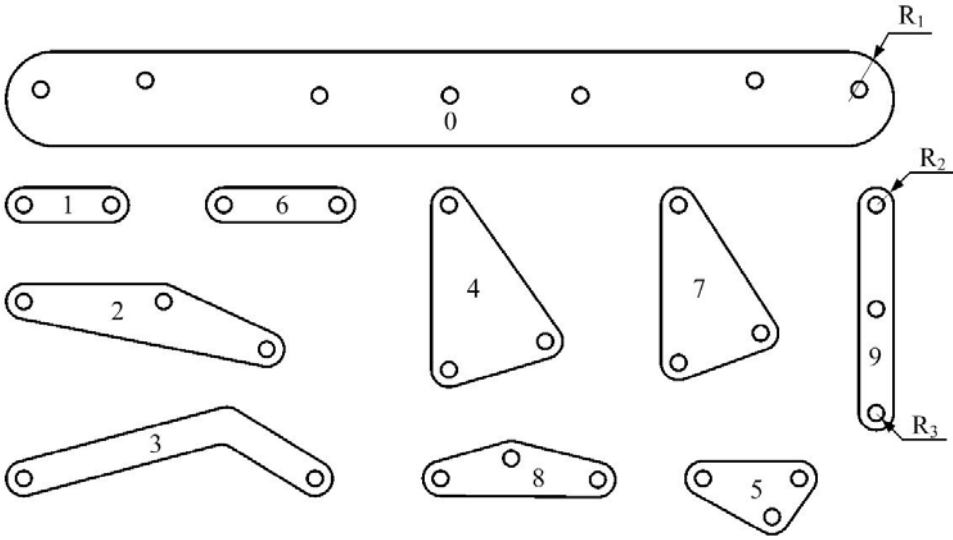
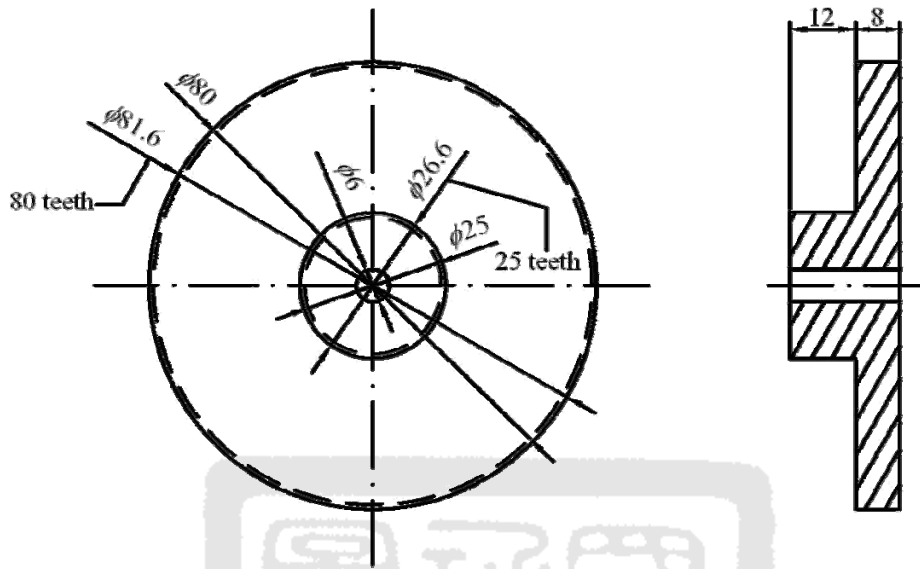
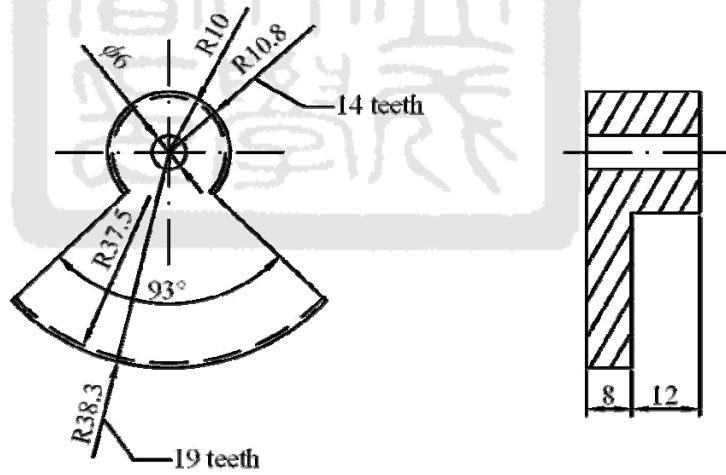


Figure 7.3 Exterior shape of each link



(a) Double-layer spur gear



(b) Fan-shaped gear

Figure 7.4 Drawings for detail designs of gears

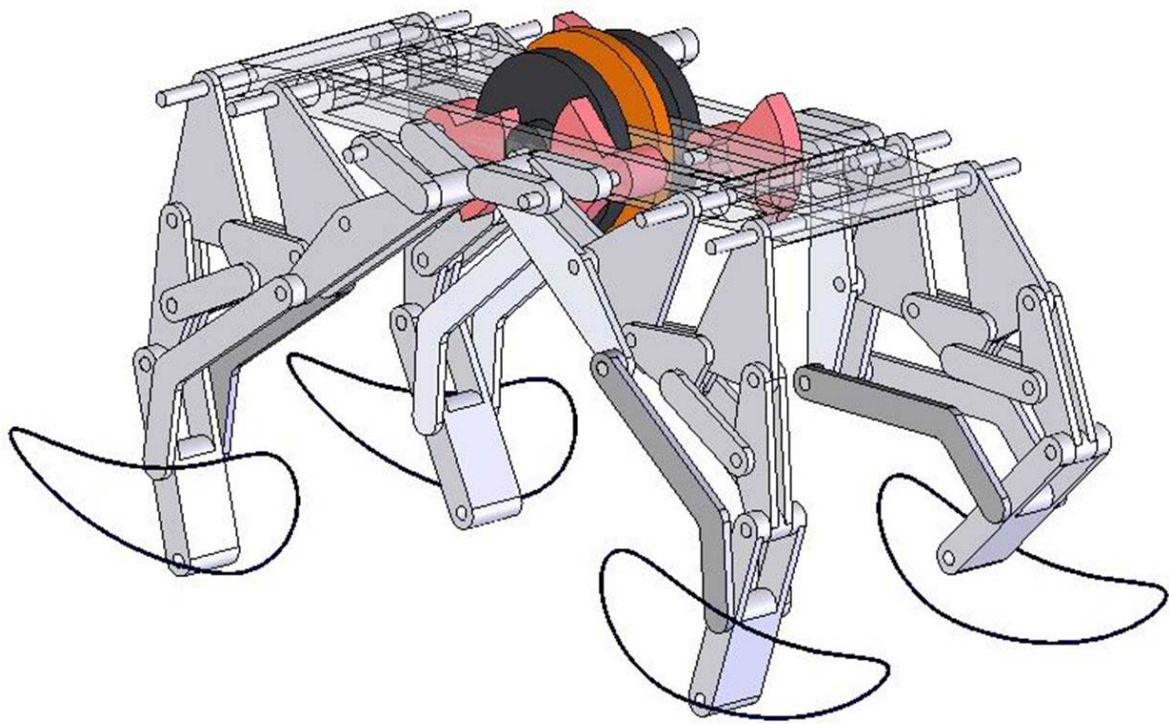


Figure 7.5 Assembly of the designed walking machine

7.3 Computer Simulation

Through computer simulation, we could check the layer arrangement and see whether any interference happens during motion. On the basis of the layer arrangement and detail link design, the model of the new walking machine with 10-bar leg mechanism for simulation is built up by using the software, SolidWorks 2005. After building up the model, the animation for simulation of the walking machine is made eventually and shown in Fig. 7.6 for several successive pictures.

7.4 Prototype

The links of the prototype of the new walking machine is fabricated with acryl by a NC machining center. The gears are made up of the plastic steel. The driving motor rotates at the nominal speed of 300 rpm. The complete assembly of the prototype of the walking machine is shown in Fig. 7.7.

By observing the motion of the designed walking machine, it can be detected that the walking machine walks almost smoothly regardless of the undulation of the body. The vibrations of the body with the motor happen as predicted by the analysis of mechanical advantage. The impacts caused by the discontinuities of the power transmission of the fan-shaped gears also occur as predicted in Chapter 6. However, these vibrations and impacts are not the worse problems. The worse problem is that the engagements of the fan-shaped gears with the driving double-layer gears are not smooth while the big fan-shape gear shifts to the small one. Sometimes, it causes the legs out of phases and the walking machine can not keep the stability of walking. In spite of the vibrations and the disengagements, there is no influence on the stability when the new type walking machine walks, and the new type walking machine needs no carriage for balancing and stable walking.

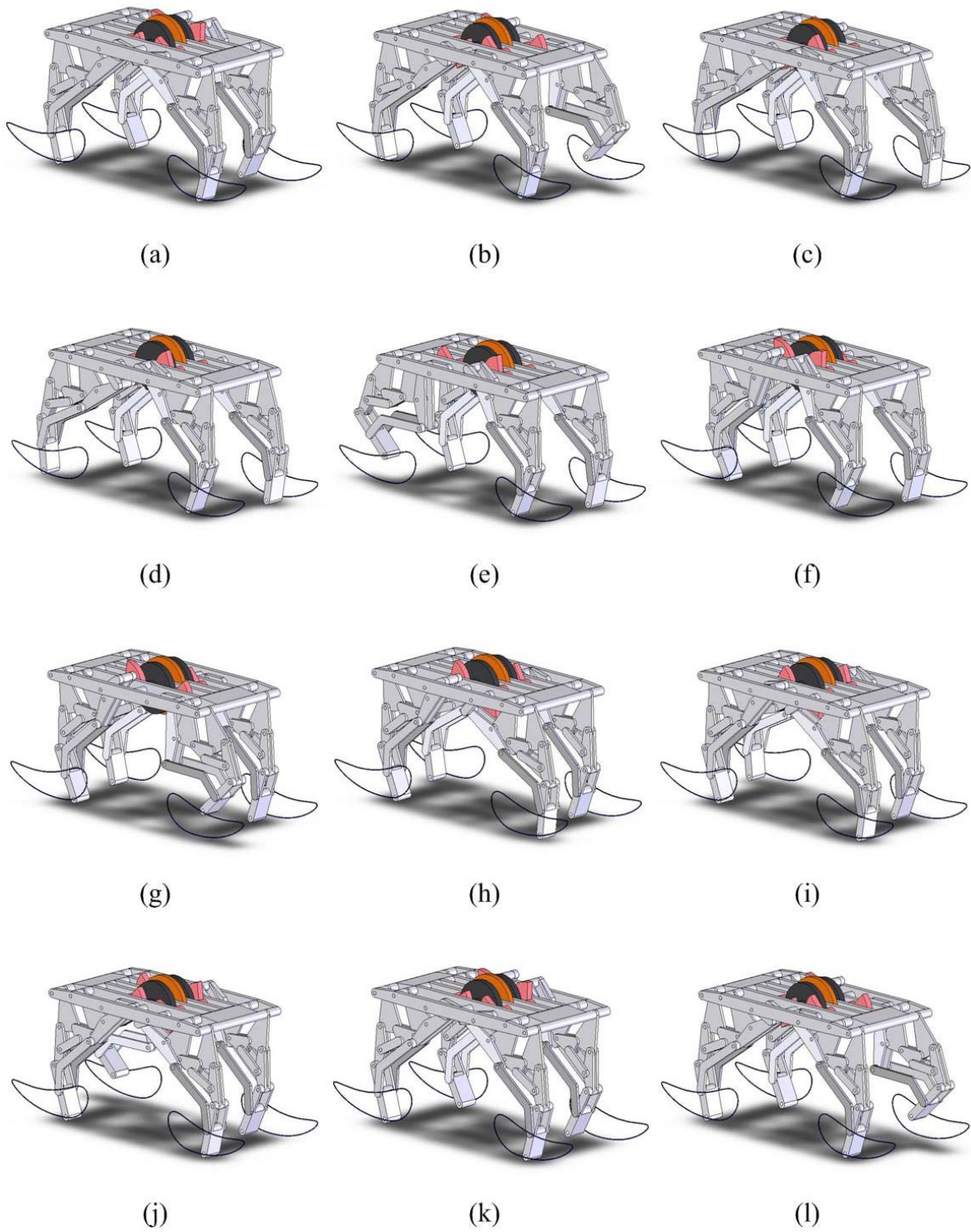


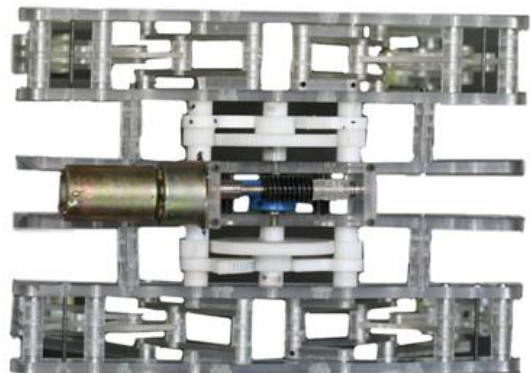
Figure 7.6 Successive pictures of animation



(a)



(b)



(c)

Figure 7.7 Prototype of the designed walking machine

Chapter 8

Conclusions and Suggestions

This work performs a research related to a self-balanced quadruped walking machine with each leg mechanism of 10-bar linkage. It includes the theoretical derivations for the synthesis of the leg mechanism, the kinematic and force analysis and the performance analysis, and the design, construction and the verification of a prototype.

The results and contributions of this works are concluded as follows:

1. In this study, a systematic design approach is applied to obtain successfully a desired path generator as the leg mechanism; and then, the path generator is utilized to construct a self-balanced quadruped walking machine with leg mechanisms of 10-bar linkage.
2. A 10-link type of leg mechanism is developed and obtained based on the leg mechanism of Chiang's wooden horse carriage, and the performances of the new designed 10-link type in several aspects are better than those of Chiang's such as the foot trajectory.
3. The kinematic analysis and force analysis of the designed walking machine is completely performed, and the walking machine is able to walk smoothly by evaluating the mechanical advantage.
4. The prototype of the new designed walking machine driven by a DC motor attached to a set of gear train is constructed, and it is able to keep stable walking without the help of the carriage.
5. The prototype does not have good energy efficiency due to vertical variation of the CG while walking on flat ground in order to have excellent ability of obstacle-crossing. By the same reason, the impact force produced at the moment when the transferring leg lands on the ground is increased.
6. The concept of two-speed control is imposed on the crank of a leg mechanism to increase the duty factor. Using the fan-shaped gear pairs makes this concept feasible.

7. The number of links of this 10-link type walking is more than those of 4-link type, 6-link type, or 8-link type, so the interferences between links are much more complicated. In order to reduce the friction between links and joints to make the theoretical analysis more compatible with real practice, more efforts should be taken on the layer arrangement and on the lubrication between links and joints

The following relevant works and suggestions that are worth for future studying:

1. In this study, a systematic design approach is applied to obtain successfully a desired path generator as the leg mechanism; and then, the path generator is utilized to construct a self-balanced quadruped walking machine with leg mechanisms of 10-bar linkage.
2. In this study, the (10, 13) kinematic chains with binary links and ternary links are concerned. The feasible leg mechanisms with better performance may be constructed by the (10, 13) kinematic chains with multiple links of more than three incident joints.
3. The gait using in this study is only focused on the amble or walk. The other types of gaits such as trot, canter, and gallop can be used to design the legged vehicles with rapid locomotion speed.
4. While designing the leg mechanism, the foot trajectory and the gait are concerned without regarding to other biological characteristics of living animals. The biological behaviors could be considered in future study.
5. The designed walking machine is only able to walk straight forwards. Applying other types of kinematic pairs except revolute pairs may obtain the designs that are able to change the direction of motion.
6. When choosing the driving motor of the prototype, the rational speed of the motor is considered in this study. However, the torque and the output power of the motor are important and should be taken into account. The result of force analysis is useful and helpful for the considerations of torque and output power.
7. The method of two-speed control is an important part to maintain the statically stable while walking, and the fan-shaped gear plays a major role on the two-speed control. However, it is difficult to confirm the engagement of gears when one fan-shaped gear shifts to the other, and thus the locomotion pauses. There should be a better method to achieve the two-speed control.

References

- [1] Song, S. M. and Waldron, K. J., *Machines that Walk: the Adaptive Suspension Vehicle*, MIT Press, London, 1989.
- [2] Rygg, L. A., "Mechanical Horse," U.S. Patent 491,927, 1893.
- [3] Shigley, J. E., "The Mechanics of Walking Vehicles," *Land Locomotion Laboratory Report No. LL-71, U.S. Army Tank-Automotive Command, Warren, Michigan, September 1960.*
- [4] McGhee, R. B., "Finite State Control of Quadruped Locomotion," *Proceedings of Second International Symposium on External Control of Human Extremities, Dubrovnik, Yugoslavis, August 1966.*
- [5] Hirose, S., "A Study of Design and Control of a Quadruped Walking Vehicle," *The International Journal of Robotics Research*, Vol. 3, No. 2, pp. 113-133, 1984.
- [6] Raibert, M. H., Chepponis, M., and Brown, H. B., "Running on Four Legs as Though They Were One," *IEEE Journal of Robotics and Automation*, Vol. RA-2, No.2, pp. 70-82, 1986.
- [7] Yan, H. S., "*I am working like a horse and an oxen (in Chinese)*," *Engineering (Taipei)*, Vol. 68, No. 10, pp. 17-25, 1995.
- [8] Yan, H. S., *Creative Design of Mechanical Devices*, Springer, Singapore, 1998.
- [9] Chen, P. H., *On the Mechanism Design of 4-link and 6-link Types Wooden Horse Carriages (in Chinese)*, M. S. thesis, National Cheng Kung University, Tainan, Taiwan, R.O.C., 1998.
- [10] Chiu, C. P., *On the Design of a Wave Gait Walking Horse (in Chinese)*, M. S. thesis, National Cheng Kung University, Tainan, Taiwan, R.O.C., 1996.
- [11] Hwang, K., *On the Design of an Optimal 8-link Type Walking Horse (in Chinese)*, M. S. thesis, National Cheng Kung University, Tainan, Taiwan, R.O.C., 1997.
- [12] Shen, H. W., *On the Mechanism Design of 8-link Type Walking Horses (in Chinese)*, M. S. thesis, National Cheng Kung University, Tainan, Taiwan, R.O.C., 1999.
- [13] Hung, C. C., *On the Mechanism Design of A Hybrid 8-link Type Walking Horse (in Chinese)*, M. S. thesis, National Cheng Kung University, Tainan, Taiwan, R.O.C., 2002.
- [14] Chiang, K. C., *A Reconstruction Design of Lu-Ban's Wooden Horse Carriage with*

- 10-bar Linkages* (in Chinese), M. S. thesis, National Cheng Kung University, Tainan, Taiwan, R.O.C., 2004.
- [15] Song, S. M., *Kinematic Optimal Design of a Six-Legged Walking Machine*, Ph. D. dissertation, The Ohio State University, Columbus, Ohio, 1984.
- [16] McGhee, R. B., “Some Finite State Aspects of Legged Locomotion,” *Mathematical Biosciences*, Vol. 2, pp. 67-84, 1968.
- [17] McGhee, R. B. and Frank, A. A., “On the Stability Properties of Quadruped Creeping Gaits,” *Mathematical Biosciences*, Vol.3, pp. 331-351, 1968.
- [18] Muybridge, E., *Animals in Motion*, New Dover Edition, Dover Publications, Inc., New York, 1957.
- [19] Butler D., *The Principles of Horseshoeing II*, Revised and Enlarged Edition, Doug Butler Publisher, Maryville, Missouri, 1985.
- [20] Alexander, R. M., “The Gaits of Bipedal and Quadrupedal Animals,” *The International Journal of Robotics Research*, Vol. 3, No. 2, pp. 49-59, 1984.
- [21] Alexander, R. M., *Exploring Biomechanics: Animals in Motion*, Scientific American Library, New York, 1992.
- [22] Edwards, E. H., *The Ultimate Horse Book*, Dorling Kindersley, Inc., New York, 1991.
- [23] Seddon, T., *Animal Movement*, Facts On File, Inc., New York, 1988.
- [24] Chen, Y. G., “An Approach to Design a Quadruped Walking Machine with a Single Actuator,” *Transactions of Canadian Society for Mechanical Engineering*, Vol. 27, No.4, pp.353-374, 2004.
- [25] Yan, H. S., *Mechanisms* (in Chinese), 2nd Ed., Tung Hua Books, Taipei, pp. 71-72, 1999.
- [26] Rao, S. S., *Engineering Optimization—Theory and Practice*, 3rd Ed., John Wiley & Sons, Inc., U.S.A., pp. 521-529, 1996.
- [27] Norton, R. L., *Design of Machinery—An Introduction to the Synthesis and Analysis of Mechanisms and Machines*, 3rd Ed., McGraw Hill, New York, pp. 559-607, 2004.
- [28] Hall, A. S. Jr., *Notes on Mechanism Analysis*, Balt Publishers, Lafayette, Indiana, 1981.
- [29] Erdman, A. G. and Sandor, G. N., *Mechanism Design—Analysis and Synthesis*, Vol. 1, 3rd Ed., Prentice-Hall International, New Jersey, pp. 165-176, 1997.
- [30] Liao, Y. H., *Optimal Arrangement of Planar Linkages with Minimum Layers* (in

Chinese), M. S. thesis, National Cheng Kung University, Tainan, Taiwan, R.O.C., 1993.

VITA

Chih-Yung Huang

Birth: July 28, 1982

Kaohsiung County, TAIWAN (R.O.C.)

Address: No. 14, Dongchang St., Jiouru Township,

Pingtung County 904, Taiwan (R.O.C.)

Telephone: 886(8)739-4802

E-mail: fleo1006@hotmail.com

Education: 2000.09 ~ 2004.06 Bachelor of Science

Department of Mechanical Engineering

National Cheng Kung University, Tainan, TAIWAN

2004.09 ~ 2006.06 Master of Science

Department of Mechanical Engineering

National Cheng Kung University, Tainan, TAIWAN

自述

姓 名：黃智勇

生 日：民國 71 年 7 月 28 日

籍 貫：台灣省高雄縣

學 歷：國立成功大學機械工程研究所碩士班

（民國 93 年 9 月至民國 95 年 6 月）

國立成功大學機械工程學系學士

（民國 89 年 9 月至民國 93 年 6 月）

通訊地址：904 屏東縣九如鄉東寧村東昌街 14 號

聯絡電話：(08)739-4802

電子信箱：fleo1006@hotmail.com

著作權聲明(Copyright Statement)

本論文非經顏鴻森教授同意不得影印。

The material contained in this thesis cannot be copied without the permission from Professor Hong-Sen Yan.

Signature (簽章) 